Energy Reports 12 (2024) 4055–4075

Contents lists available at ScienceDirect

Energy Reports

journal homepage: www.elsevier.com/locate/egyr

Review article

# Overview of superconducting wireless power transfer

Rui Lyu [a], Wei Liu [b], Quan Li [c], K.T. Chau [b,*]

[a] Department of Electrical and Electronic Engineering, The University of Hong Kong, Hong Kong, China
[b] Research Centre for Electric Vehicles and Department of Electrical and Electronic Engineering, The Hong Kong Polytechnic University, Hong Kong, China
[c] ENN Science and Technology Development Co., Ltd., Hebei, China

A R T I C L E I N F O

*Keywords:*
Wireless power transfer
High-temperature superconducting
HTS inductor
HTS capacitor

A B S T R A C T

Wireless power transfer (WPT) technology has received much attention due to its flexibility and safety, becoming an important area of research and development for various applications. However, conventional WPT systems are often constrained by the inherent properties of physical circuit components, leading to limitations in power density and transmission efficiency. The advent of high-temperature superconducting (HTS) materials offers a promising pathway to significantly enhance WPT performance by leveraging the nearly zero resistance and higher current-carrying capacity of HTS materials. This review comprehensively examines the state-of-the-art in HTS devices and HTS-based wireless power transfer (HTS-WPT) technology. By systematically analyzing the theoretical and experimental advances in HTS-WPT systems, this review aims to provide a comprehensive understanding of their advantages and limitations, offering insights for future research and practical implementations in various promising applications.

## 1. Introduction

Since Nikola Tesla introduced the concept of cordless electric energy transfer (Tesla, 1904, 1914), wireless power transfer (WPT) technology has received widespread attention for its flexibility and safety, and has become one of the most attractive research hotspots in recent years (Kurs et al., 2007; Assawaworrarit et al., 2017; Lerosey, 2017; Qiu et al., 2013). Among various WPT technologies, inductively coupled magnetic resonant WPT is widely regarded as one of the most effective solutions, offering superior performance in terms of power capacity, energy efficiency, flexibility, and safety compared to other WPT technologies (Liu et al., 2023). It is now widely applied in fields such as transportation (Mi et al., 2016), energy (Liu et al., 2022a), information (Basir and Yoo, 2020), and medicine (Haerinia and Shadid, 2020), ranging from numerous low-power portable electronic components to high-power applications exceeding 200 kW, including electric buses and ferries (Martha's vineyard buses get wirelessly charged up with 200-kW system, 2018; Wireless charging for a smooth and safe power transfer from shore to the ferry, 2019). However, the system performance of conventional WPT systems is constrained by the inherent properties of commonly used metallic materials (Bosshard et al., 2015). The reduction in system size may directly lead to a decrease in transmission efficiency and maximum transmission power. Consequently, conventional high-power WPT systems are typically limited to heavy machinery applications, while suitable alternatives are needed for applications with stringent size and weight constraints.

The advent of superconducting materials offers a promising solution to break through the performance limitations of conventional WPT systems. The phenomenon of superconductivity was first documented in 1911 by Dutch scientist Heike Kamerlingh-Onnes, when he observed that the resistance of mercury dropped dramatically to zero when it was cooled to a temperature of 4.2 K, which is equivalent to that of liquid helium (LHe) (Kamerlingh Onnes, 1911). Following this groundbreaking discovery, in 1933, German scientists Walther Meissner and Robert Ochsenfeld discovered the complete diamagnetism of superconducting materials, a property where superconducting materials expel all magnetic flux lines from the inside, which is known as the Meissner effect (Meissner and Ochsenfeld, 1933). Leveraging the perfect conductivity and complete diamagnetism of superconducting materials, superconducting circuit components can be manufactured to replace conventional circuit components in WPT systems, which can help to overcome the limitations of material properties, achieving better WPT performance (Chen and Jin, 2011; Kim et al., 2012). Considering the cost of cooling materials, high-temperature superconducting (HTS) materials, which exhibit superconductivity at liquid nitrogen ($LN_2$) temperatures, are more favoured by researchers compared to low-temperature superconducting (LTS) materials, which require

* Corresponding author.
*E-mail address:* k.t.chau@polyu.edu.hk (K.T. Chau).

https://doi.org/10.1016/j.egyr.2024.09.067
Received 8 July 2024; Received in revised form 28 August 2024; Accepted 27 September 2024
Available online 7 October 2024

**Nomenclature**

| | |
|---|---|
| AC | alternating current |
| Ag | silver |
| BSCCO | bismuth-based cuprate superconductingmaterials |
| CC | coated conductors |
| Cu | copper |
| DC | direct current |
| EV | electric vehicle |
| HF | high frequency |
| HTS | high-temperature superconducting |
| IBS | iron-based superconducting materials |
| IGBT | insulated gate bipolar transistors |
| $LH_2$ | liquid hydrogen |
| LHe | liquid helium |
| $LN_2$ | liquid nitrogen |
| LTS | low-temperature superconducting |
| MOSFET | metal-oxide-semiconductor field-effect transistors |
| MRI | magnetic resonance imaging |
| PIT | powder-in-tube |
| REBCO | rare-earth barium copper oxide superconducting materials |
| WPT | wireless power transfer |
| $H_c$ | critical magnetic field strength |
| $J_c$ | critical current density |
| $T_c$ | transition temperature |
| $k$ | coupling coefficient |
| $Q$ | quality factor |

cooling to liquid hydrogen ($LH_2$) or even LHe temperatures (Chow et al., 2023).

This review primarily focuses on HTS-based inductively coupled magnetic resonance wireless power transfer (HTS-WPT) systems. A comparison of conventional WPT systems with HTS-WPT systems is shown in Fig. 1. Compared to conventional WPT systems, HTS-WPT systems leverage the nearly zero resistance and higher current-carrying capacity of HTS circuit components to establish stronger magnetic field coupling between the transmitter and receiver while minimizing circuit losses. This results in superior system performance with reduced volume and weight. However, achieving the exceptional performance of HTS-WPT systems while ensuring their stability and reliability involves more than simply replacing conventional circuit components with HTS elements; numerous practical challenges must be addressed. Due to the high operating frequencies of WPT systems, HTS materials experience notable alternating current (AC) losses when high frequency (HF) currents flow through them, dissipating as heat into the environment (Zhang et al., 2013). To maintain the low-temperature conditions necessary for superconductivity, additional cooling apparatus is required, which consumes non-negligible extra power. Without adequate cooling, the HTS components risk losing their superconducting properties. The installation of cooling systems increases the overall complexity of the system, and the power required for cooling can diminish the overall performance, thereby jeopardizing the advantages

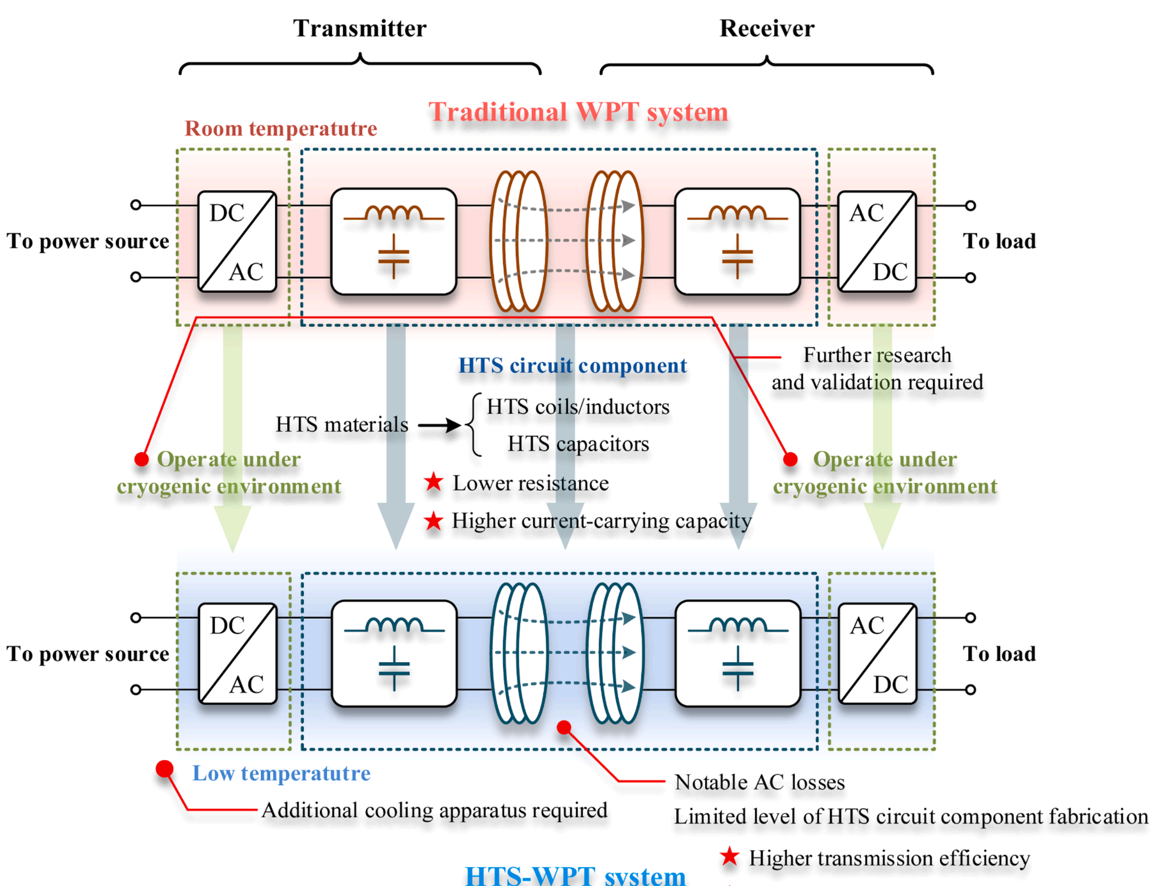


**Fig. 1.** Comparison of conventional WPT system with HTS-WPT system.

of HTS-WPT systems (Machura et al., 2020). Furthermore, the current level of HTS circuit component fabrication poses a major bottleneck in the development of HTS-WPT systems (Sekiya and Monjugawa, 2017; Sekiya and Sawada, 2023). Additionally, the operational characteristics of other circuit components within the system under low-temperature conditions require further research and validation (Gui et al., 2019). As shown in Fig. 2, over the past few years, an increasing number of theoretical and experimental studies on HTS-WPT systems have been conducted, yielding significant insights into their system characteristics, advantages, and limitations. This review systematically and comprehensively examines these studies, aiming to provide a thorough understanding of HTS-WPT systems and outline a blueprint for future research and practical applications.

The article is organised as follows. Section 2 will introduce the characteristics, applications, and recent developments of HTS devices, including HTS materials, HTS inductors, and HTS capacitors. Section 3 will review the relevant research on HTS-WPT systems and summarize potential applications based on their characteristics. Section 4 will discuss the development trends and existing limitations of HTS-WPT systems. Finally, Section 5 will conclude this review.

## 2. HTS devices

### 2.1. HTS Materials

Initial studies on superconducting materials revealed that maintaining a superconducting state is contingent upon satisfying three fundamental conditions, as shown in Fig. 3. Firstly, the ambient temperature must be below the transition temperature $T_c$; secondly, the applied magnetic field should remain below the critical magnetic field strength $H_c$; and thirdly, the current flowing through the superconducting material should not exceed its maximum current-carrying capability, known as the critical current density $J_c$ (Tinkham, 2004). Different superconducting materials exhibit significant variations in the three critical parameters, which are pivotal for the practical applications of superconducting materials. Collectively, to date, thousands of superconducting materials have been identified, which can be broadly classified based on their $T_c$ into two categories: LTS materials and HTS materials.

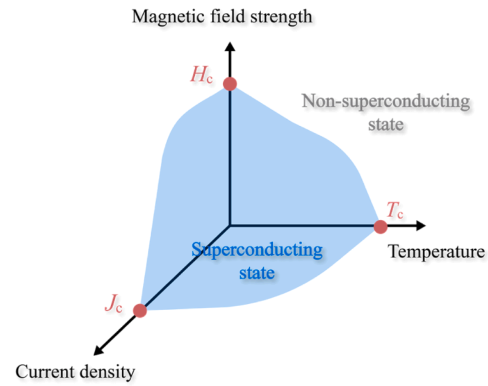


**Fig. 3.** Superconducting state diagram.

This classification stems from the principles set forth by the BCS theory, proposed in 1957 by John Bardeen, Leon Cooper, and Robert Schrieffer (Bardeen et al., 1957). The BCS theory, grounded in quantum mechanics and condensed matter physics, describes how electrons in superconducting materials pair up to form Cooper pairs, leading to the complete disappearance of electrical resistance. This theory elegantly explains the perfect electrical conductivity and complete diamagnetism observed in LTS materials, providing a crucial foundation for the study and application of superconductivity. However, it fails to account for the behaviours of superconducting materials with $T_c$ above 30 K. Thus, a $T_c$ of 30 K serves as the dividing line between LTS materials and HTS materials.

Mercury, recognized as the first discovered superconducting material, has a $T_c$ of 4.2 K, marking the initial discovery of LTS materials. Over the subsequent decades, numerous metals, alloys, and intermetallic compounds exhibiting superconductivity have been discovered. Among these, Nb-Ti and $Nb_3Sn$ reported in 1954 and 1961 respectively, are the most extensively used LTS materials to date (Rogalla and Kes,

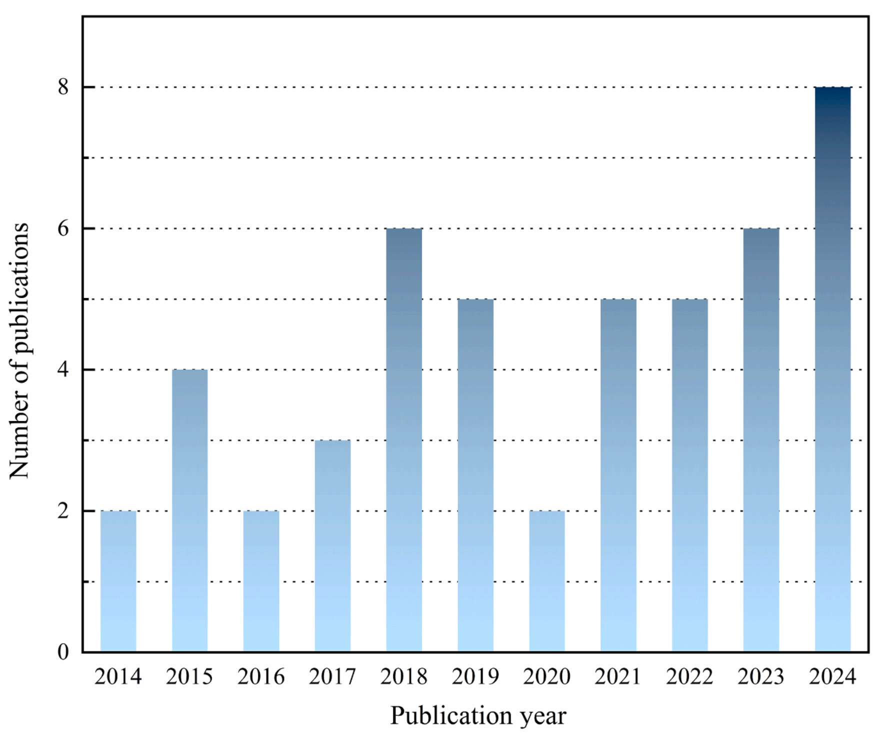


**Fig. 2.** Annual publications regarding HTS-WPT technologies in IEEE Xplore, MDPI, and Springer, dated between inception and June 18th, 2024.

2012). Nb-Ti, an alloy, exhibits a $T_c$ of 9.5 K and can achieve a $J_c$ exceeding 2000 A/mm$^2$ at 4.2 K, with an $H_c$ of approximately 11 T (Lee, 2018). Due to its excellent ductility, Nb-Ti alloy is relatively easy to manufacture into superconducting wires and was industrialized in 1968. Currently, Nb-Ti remains the most cost-effective LTS material, extensively used in constructing magnetic resonance imaging (MRI) systems and maglev trains. In contrast, $Nb_3Sn$, an intermetallic compound, has a $T_c$ of around 18 K and can reach a $J_c$ of over $10^4$ A/mm$^2$ at 4.2 K, with an $H_c$ of about 25 T (Lee, 2018). Compared to Nb-Ti, $Nb_3Sn$, due to its brittleness, presents more complexities in the wire manufacturing process and was industrialized after 1970; however, it is more expensive. Owing to its higher $H_c$, $Nb_3Sn$ is primarily used in applications requiring higher magnetic fields, such as particle accelerators and tokamak fusion devices.

In 1986, Johannes Georg Bednorz and Karl Alexander Müller reported the first HTS material, LaBaCuO, with a $T_c$ of 35 K, sparking widespread research into HTS materials (Bednorz and Muller, 1986). The following year, 1987, the HTS material YBCO was reported, achieving a $T_c$ of 93 K. This marked the first instance of a superconducting material's $T_c$ surpassing the temperature of $LN_2$, which is approximately 77 K (Zhao et al., 1987; Wu et al., 1987). In the same year, the bismuth-based cuprate superconducting materials (BSCCO), Bi-2212 and Bi-2223 were reported, with $T_c$ reaching up to 110 K (Michel et al., 1987). YBCO is a type of rare earth barium copper (Cu) oxide superconducting materials (REBCO) and both REBCO and BSCCO belong to the family of Cu oxide superconducting materials, characterized by their high $T_c$, allowing them to maintain a superconducting state at the temperature of $LN_2$. Given the abundant availability of nitrogen compared to helium, using $LN_2$ for cooling is much more cost-effective. However, due to the brittleness of these materials, they are more challenging to process into wires compared to LTS materials. BSCCO and REBCO were not successfully manufactured on an industrial scale until the 1990s and after 2000, respectively (Uglietti, 2019). So far BSCCO tapes have been widely used in various superconducting power equipment demonstration projects around the world, such as power cables, superconducting energy storage devices, and fault current limiters (Sato et al., 2012; Xiao et al., 2012). Compared to BSCCO, REBCO exhibit lower anisotropy and a higher $J_c$ at 77 K, and it have been utilized in numerous superconducting power devices to optimize electrical systems and in the manufacturing of high-field Tesla magnets to pursue new records in magnetic fields (Obradors and Puig, 2014; Liu et al., 2020). These applications highlight REBCO's tremendous potential.

In 2001, $MgB_2$ was reported, making it the binary intermetallic compound with the highest known $T_c$ at that time, reaching up to 39 K (Nagamatsu et al., 2001). Although this is still lower than that of Cu oxide superconducting materials, $MgB_2$ can maintain superconductivity at the temperature of $LH_2$, making it a potentially ideal alternative to conventional LTS materials that require LHe. Additionally, $MgB_2$ is characterized by its abundant raw materials, lightweight nature, and relatively easy wire fabrication process, which have attracted widespread attention in the scientific community. Compared to the cost of REBCO, which is approximately 230 \$/(kA·m), the manufacturing cost of $MgB_2$ is considerably lower, around 20 \$/(kA·m) (Uglietti, 2019). In contrast, Cu materials cost about 11.6 \$/kg. Given that the rated current density for Cu wires usually does not exceed 10 A/mm$^2$, the cost of Cu wire is approximately 10.4 \$/(kA·m). Therefore, the discovery of $MgB_2$ material holds promise for significantly reducing the cost of HTS materials, thereby promoting the widespread application of HTS technologies. However, due to a lack of pinning centers within the material, the $J_c$ of $MgB_2$ under high magnetic fields is severely limited (Dou et al., 2002). As a result, its primary applications are currently in low magnetic field areas such as fault current limiters, power cables, and wind turbines.

In 2008, iron-based superconducting materials (IBS) were reported with $T_c$ reaching up to 56 K (Kamihara et al., 2008). Although these $T_c$ values are significantly lower than those of cuprate superconducting materials, IBS exhibit high $H_c$ and notably lower anisotropy. Research on the grain boundary properties in IBS has highlighted the potential of the low-cost powder-in-tube (PIT) method, which has been successfully applied in the commercial production of $Nb_3Sn$, Bi-2223, and $MgB_2$ wires (Katase et al., 2011). Consequently, IBS wires developed using the PIT method are promising due to their low cost and high strength, indicating a bright future for applications. Currently, IBS materials are still in the experimental research stage, and they hold potential as materials for high magnetic field applications such as magnets in high-energy accelerators (Zhang et al., 2021a).

In recent years, there have been reports concerning materials that exhibit superconducting-like properties at room temperature under extremely high pressures (Snider et al., 2020). However, the classification of these materials as true superconducting materials remains uncertain (Hirsch and Marsiglio, 2021). Moreover, the necessity of maintaining such high pressures to achieve these properties at room temperature poses significant challenges for practical engineering applications. Therefore, this article will not discuss these materials in detail.

Based on the preceding discussion, the discovery dates and $T_c$ of some landmark superconducting materials are depicted in Fig. 4. Table 1 illustrates the conductor forms of practical superconducting materials. Table 2 provides a comprehensive summary of the critical parameters, key features, and commercialization status of these materials. As shown in the table, HTS materials offer considerable advantages over LTS materials, including higher $T_c$ and $H_c$. Therefore, HTS materials are more advantageous for use in WPT systems, where high efficiency and power density are crucial.

### 2.2. HTS inductors

Inductors, which are integral components within power electronic circuits, fulfil several critical roles including filtering, energy storage, and moderating the rate of change of current. With the ongoing advancements in power circuit technology, there has been an increasing emphasis on enhancing both efficiency and power density (Zhao et al., 2014). Consequently, inductors have been developed towards smaller size, reduced losses, and higher saturation current capabilities. Nevertheless, conventional inductors are manufactured by winding Cu wire around a magnetic core, which presents certain limitations. Firstly, Cu wire inherently exhibits low current density and introduces significant parasitic resistance. Secondly, in HF applications, the magnetic core is prone to considerable hysteresis and eddy current losses. Additionally, skin and proximity effects further exacerbate Cu losses. These issues collectively pose substantial barriers to achieving higher efficiency and power density in power electronic circuits.

Like many other metals, Cu exhibits lower resistivity at reduced temperatures. Many studies have explored the low-temperature operation of conventional Cu inductors (Gui et al., 2019; Dionne, 1997; Chen et al., 2018; Wadsworth et al., 2023). Research on HF core materials has revealed that only high-flux powder cores maintain relatively stable magnetic permeability and loss characteristics at low temperatures, whereas the performance of other core materials deteriorates, as indicated in Table 3 (Chen et al., 2003; Gerber et al., 2004; Quach and Chui, 2004; Claassen, 2005; Willard and Heil, 2007; Daniil et al., 2010, 2015). On the one hand, the reduction in magnetic permeability may necessitate increased core volume, adversely affecting power density. On the other hand, increased losses not only reduce system efficiency but also require additional power consumption to maintain a low-temperature environment. One solution is to use air-core inductors, which are wound without a magnetic core. Studies documented in (Park et al., 2020) have investigated the performance of air-core Cu inductors carrying direct current (DC) at 77 K, finding that their parasitic resistance is significantly lower—about one-tenth of that at room temperature—thus allowing for a notable increase in power density. However, when carrying HF AC, the parasitic resistance may significantly increase due to

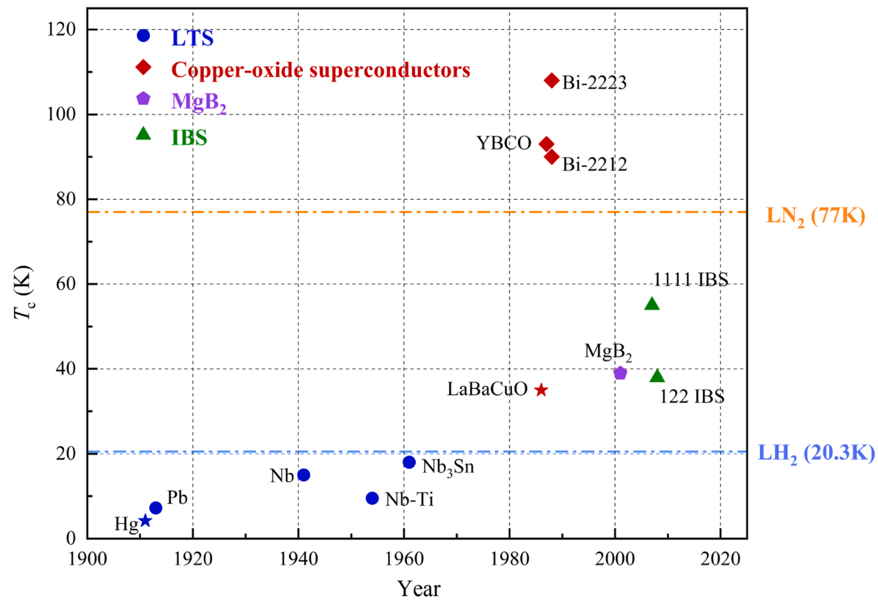


**Fig. 4.** Discovery dates and $T_c$ of some landmark superconducting materials.

the skin effect, leading to heat generation that adversely impacts the performance of air-core inductors.

Compared to conventional Cu wire inductors, HTS inductors exhibit significantly higher current density and lower losses at cryogenic temperatures, facilitating the achievement of higher efficiency and power density (Chen et al., 2016a). HTS inductors (or HTS coils) are already widely used in high-power applications such as superconducting energy storage systems, superconducting fault current limiters, and superconducting power transformers (Chen et al., 2021; Zheng et al., 2023; Kumar et al., 2023). These HTS inductors are characterized by their ability to handle large currents, operate at low frequencies (50–60 Hz), and provide substantial inductance.

However, the application of HTS inductors in HF power electronic circuits is still in the experimental research phase (Chen et al., 2016a). introduced the concept of using HTS inductors in boost converters, and a simulation study of a 40 kW system with a switching frequency below 500 Hz demonstrated the superiority of HTS inductors over conventional inductors. Following this concept, studies in (Chen et al., 2022) and (Garcia et al., 2024) conducted experiments at power levels of 1 kW to 4 kW and under 100 W, with switching frequencies of 1 kHz to 10 kHz and 3.92 kHz, respectively. The results from these studies confirmed that employing HTS inductors in boost converters significantly enhances efficiency, power density, and voltage gain. Additionally, (ul Hassan et al., 2022) explored the use of HTS inductors in a two-level current source inverter for all-electric aircraft operating at cryogenic temperatures, conducting a 20 kW/30 kHz experiment which demonstrated the effectiveness of HTS inductors in enhancing efficiency and power density.

Nevertheless, for WPT systems, which commonly operate at switching frequencies above 85 kHz—significantly higher than those used in the aforementioned HF power electronic circuits—it is crucial to consider the AC losses of HTS materials at such elevated frequencies.

Based on their underlying mechanisms, AC losses in superconducting materials can be divided into transport current losses and magnetization losses. Transport current losses occur solely due to the current carried by the superconductor and do not require an external magnetic field. Magnetization losses, on the other hand, are induced solely by the external magnetic field acting on the superconductor without the necessity of a current. Furthermore, magnetization losses can be subdivided into eddy current losses, hysteresis losses, and coupling losses, which are associated with the flux pinning in superconductors, eddy currents induced by external magnetic fields within the superconductors, and the flow of these currents in multifilamentary superconductors, respectively (Zhang et al., 2021b).

In the context of WPT systems, transport current losses and magnetization losses, especially eddy current losses and hysteresis losses, play a dominant role in overall AC losses (Zhang et al., 2013). The issue of AC losses in WPT systems is complex, which is affected by a number of factors, such as switching frequency, current magnitude, magnetic field strength and material properties. Studies in (Chen and Li, 2020) and (Utschick et al., 2021) show that both transport current losses and eddy current losses are positively correlated with frequency, while hysteresis losses are frequency-independent. This suggests that AC losses can be particularly significant at higher frequencies in WPT systems (Machura et al., 2020; Weng et al., 2024). investigated the effect of external magnetic fields and current magnitude on AC losses and showed that both parameters are positively correlated with AC losses. Furthermore, (Machura et al., 2020) analysed the effect of coil configuration on AC losses and quantitatively compared the main types of losses for different coil configurations (Utschick et al., 2021; Machura and Li, 2021). also explored how coil parameters such as air gaps, thickness, and width affect AC losses, offering guidance for the structural design of superconducting coils. In (Inoue et al., 2017), comparisons between YBCO tape and Bi2223 tape in WPT systems demonstrated that YBCO tape exhibits lower AC losses. In summary, the classification and influencing factors of superconducting coils are illustrated in Fig. 5. Compared to conventional WPT systems, quantifying and controlling AC losses is critical because the resulting heat increases the burden on cooling systems, further reducing system efficiency.

### 2.3. HTS capacitors

Although HTS inductors offer advantages such as low losses, compact size, and high saturation current, using HTS inductors in conjunction with conventional room-temperature capacitors can lead to thermal leakage issues caused by current leads (Xiao et al., 2016). This exacerbates the burden on cooling systems and reduces the overall system efficiency. Similar to HTS inductors, HTS capacitors also exhibit lower losses, which can significantly enhance the efficiency and power density of power electronic circuits. Therefore, exploring HTS capacitors and developing fully cryogenic power electronic circuits have become ideal strategies for realizing the large-scale industrial application of HTS

**Table 1**
Illustration and unit cost for practical superconducting materials (Lee, 2018; Zhang, 2019; Osabe et al., 2019; Jiang et al., 2019; Li et al., 2013; Yao et al., 2015).

| Material | | Illustration | Reference |
|---|---|---|---|
| LTS | Nb-Ti |  | Lee, 2018 |
| | $Nb_3Sn$ |  | |
| HTS | REBCO | 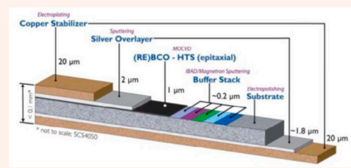  | Zhang, 2019 |
| | Bi-2223 | 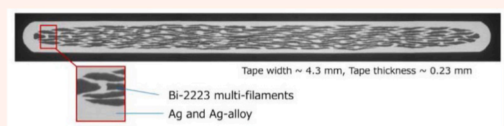  | Osabe et al., 2019 |
| | Bi-2212 |  | Jiang et al., 2019 |
| | $MgB_2$ | 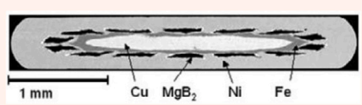   | Li et al., 2013 |
| | IBS |   | Yao et al., 2015 |

materials (Ogawa et al., 2019).

The concept of HTS capacitors was proposed as early as in 1991 (Jones et al., 1991). Similar to conventional capacitors at room temperature, HTS capacitors are composed of HTS electrodes and dielectric materials. Due to the varying properties of different dielectric materials with decreasing temperature, extensive literature has explored this issue. Common changes in capacitance values and dissipation factors of conventional capacitors at low temperatures are summarized in Table 4 (Andrade et al., 2024; Faria et al., 2012; Pan, 2005; Teyssandier and Prêle, 2010). Compared to most ceramic capacitors, film capacitors demonstrate superior performance at low temperatures. When manufacturing capacitors with larger capacitance values, tantalum capacitors are preferred over electrolytic capacitors, which tend to lose almost all their capacitance at low temperatures, although tantalum capacitors result in significantly higher losses. The use of dielectric materials in thin-film capacitors has prompted research in laboratories to explore the potential application of HTS capacitors in WPT systems. According to (Yu et al., 2019), an HTS capacitor made from Bi2223/Ag tapes and polyimide dielectric material, with a capacitance of 20 nF, was compared to conventional capacitors, showing that WPT systems utilizing HTS capacitors achieve higher efficiencies. However, the WPT experimental setup described in (Yu et al., 2019) was relatively rudimentary, achieving a peak efficiency of just under 60%. Another study in (He et al., 2018) utilized YBCO tapes as electrodes to create a 0.608 nF HTS capacitor for use in a repeater coil in a multi-stage resonant WPT system, demonstrating the advantages of HTS capacitors in enhancing power transmission capabilities in WPT systems.

The technology for manufacturing HTS capacitors capable of operating normally at high frequencies and large currents is still in its infancy. A key issue is the cold deformation of dielectric materials, which significantly impacts the lifespan of HTS capacitors. Consequently, further research is required to identify dielectric materials suitable for HTS capacitors. Additionally, to integrate HTS power electronic circuits into WPT systems, more in-depth studies are needed on the effects of current magnitude and frequency, as well as external magnetic fields, on the properties of HTS capacitors.

## 3. HTS-WPT systems

### 3.1. WPT system configurations

WPT systems offer significant advantages including convenience,

**Table 2**
Critical parameters, key features, and commercialization status of practical superconducting material.

| Classification | Material | | | $T_c$ (K) | $H_{c,\,4.2K}$ (T) | $J_{c,\,4.2K}$ (A/mm$^2$) | Anisotropy $\gamma_H$ | Key features | Commercialization status |
|---|---|---|---|---|---|---|---|---|---|
| LTS | Nb-Ti | | | 9.5 | 11 | ~$10^3$ | Negligible | LHe temperature<br>Simple and mature manufacturing process | Fully commercialised |
| LTS | $Nb_3SN$ | | | 18 | 25 | ~$10^4$ | Negligible | LHe temperature<br>Higher cost<br>Mature manufacturing process<br>Higher field applications | Fully commercialised |
| HTS | Cu-oxide superconducting materials | YBCO | | 93 | >100 | ~$10^5$ | 5-7 | $LN_2$ temperature<br>Complex manufacturing process<br>Lower anisotropy<br>Higher $J_c$<br>High-field applications | early commercialisation |
| HTS | Cu-oxide superconducting materials | BSCCO | Bi-2223 | 108 | >100 | ~$10^4$ | 50-90 | $LN_2$ temperature<br>Mature manufacturing process | early commercialisation |
| HTS | Cu-oxide superconducting materials | BSCCO | Bi-2212 | 90 | >100 | ~$10^4$ | 50-90 | $LH_2$ temperature<br>Mature manufacturing process<br>High-field applications | mid-commercialisation |
| HTS | $MgB_2$ | | | 39 | 18 | ~$10^4$ | 2-2.7 | $LH_2$ temperature<br>Mature manufacturing process<br>Abundant raw materials<br>Lightweight<br>Low-field applications only | early commercialisation |
| HTS | IBS | 1111 IBS | | 55 | >100 | ~$10^4$ | 4-5 | $LH_2$ temperature<br>Mature manufacturing process<br>Low anisotropy<br>High-field applications | not yet commercialised |
| HTS | IBS | 122 IBS | | 38 | >80 | ~$10^4$ | 1.5-2 | | |

Temperature: $LN_2$ > $LH_2$ > LHe
Data from (Lee, 2018; Yao and Ma, 2021; Parrell et al., 2003; Li et al., 2013; Kanithi et al., 2014; Song et al., 2021; Braccini et al., 2010; Gurevich, 2014; Zhang et al., 2021b)

**Table 3**
Performance of different core materials at cryogenic temperatures.

| Material | Powder | | | Ferrite | Nano-crystalline | Amorphous |
|---|---|---|---|---|---|---|
| | Moly permalloy | High flux | Kool M$\mu$ | | | |
| **Permeability** | Remain | Remain | Decrease | Significantly decrease | Increase | Remain |
| **Loss** | Increase | Remain | Remain | Significantly increase | Increase | Increase |

safety, and flexibility, which make them increasingly popular in applications ranging from mobile devices to electric vehicles (EVs). The typical structure of WPT system is illustrated in Fig. 6, which primarily consists of two subsystems: the transmitter and the receiver (Qiu et al., 2013). The transmitter subsystem includes a power source, an inverter, a compensation network, and a transmitting coil. The power source outputs an appropriate DC link voltage through a converter, which is then transformed into HF AC by the HF inverter to supply power to the coupler. Due to the inherently low quality factor of conventional Cu coils at room temperature, it is crucial to maintain high current frequencies and high coupling coefficients within the coupling coils to ensure high efficiency (Machura and Li, 2019). On the receiver side, the subsystem comprises a receiving coil, a compensation network, a rectifier, and the load. The HF AC current received by the coil is converted to the required DC output through rectification and filtering processes that powers the load.

#### 3.1.1. Coupler design

The core mechanism of WPT involves the generation of an HF AC in the transmitting coil, which produces a time-varying magnetic field to induce energy into the receiving coil. Consequently, the coupling coefficient $k$ between the transmitting and receiving coils is crucial. Moreover, the quality factor $Q$ of a coil, defined as the ratio of its reactance to resistance, quantifies the energy losses at resonance (Long et al., 2016). A higher $Q$-value indicates that a greater proportion of the energy is converted to and transmitted via the magnetic field, rather than being dissipated as heat in the coil's resistance. As such, to optimize the efficiency of WPT systems, it is essential to maximize both the $k$-value and the $Q$-value during coil design.

For conventional WPT systems, increasing $Q$-value can be achieved through methods such as increasing switching frequency and optimizing coil parameters (e.g., increasing wire diameter). However, increasing switching frequency also raises frequency-related losses, such as switching losses in converters, and core losses and resistive losses in coils. Moreover, converters designed to operate at higher switching frequencies generally incur higher costs. Regarding the operating frequency of WPT systems in EVs, standards have been issued by the International Electrotechnical Commission (IEC) and the Society of Automotive Engineers (SAE), recommending an operating frequency range of 81.38–90 kHz (Rakouth et al., 2013; Wireless Power Transfer for Light-Duty Plug-In/Electric Vehicles and Alignment Methodology, 2016). On the other hand, due to the intrinsic properties of commonly used metallic materials at room temperature, there are inherent limitations on the extent to which $Q$-value can be enhanced by optimizing coil structures (Kim et al., 2013). To enhance $k$-value, strategies such as using magnetic core materials, reducing transmission distance, and optimizing coil parameters (e.g., increasing coil area) can be employed. However, the introduction of magnetic core materials introduces

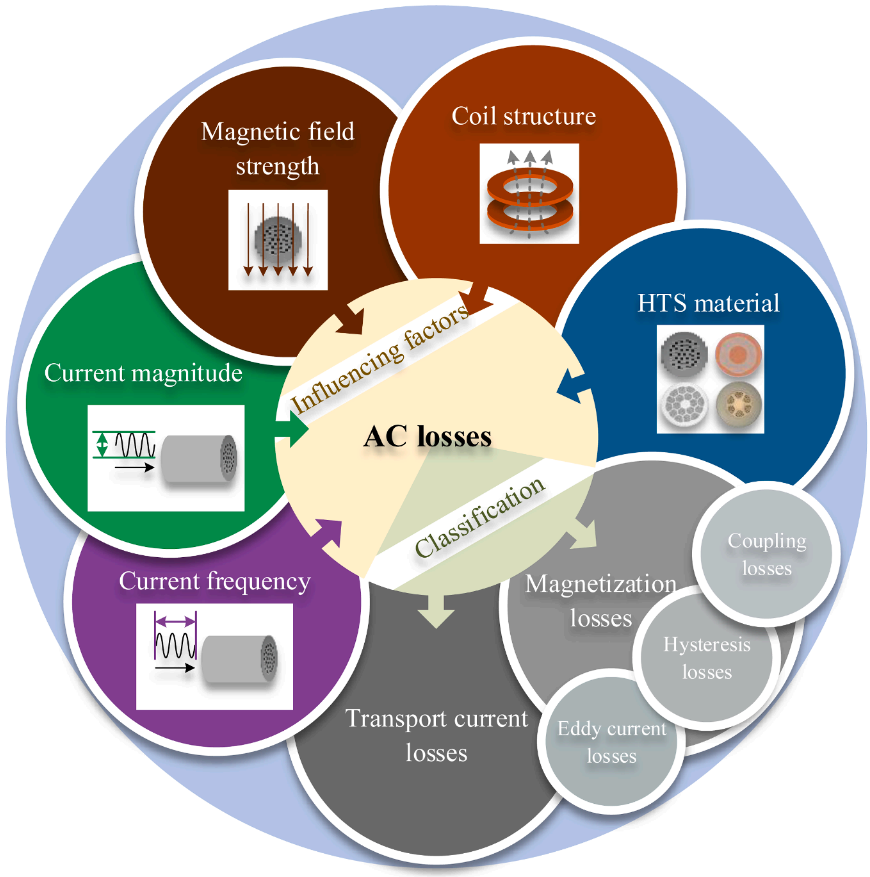


**Fig. 5.** Classification and influencing factors of AC losses in HTS coils.

**Table 4**
Performance of different dielectric materials at cryogenic temperatures.

| Material | Film | | | | |
|---|---|---|---|---|---|
| | Polypropylene | Polyester | Polycarbonate | Polyphenylene sulfide | Polyimide |
| Relative permittivity | Remain | Decrease | Decrease | Remain | Decrease |
| Dissipation factor | Decrease | Remain | Decrease | Remain | Remain |
| Material | Ceramics | | | Tantalum | Al electrolytic |
| | X7R | Z5U | NP0 | | |
| Relative permittivity | Significantly decrease | Significantly decrease | Remain | Decrease | Significantly decrease |
| Dissipation factor | Significantly increase | Significantly increase | Remain | Significantly increase | Decrease |

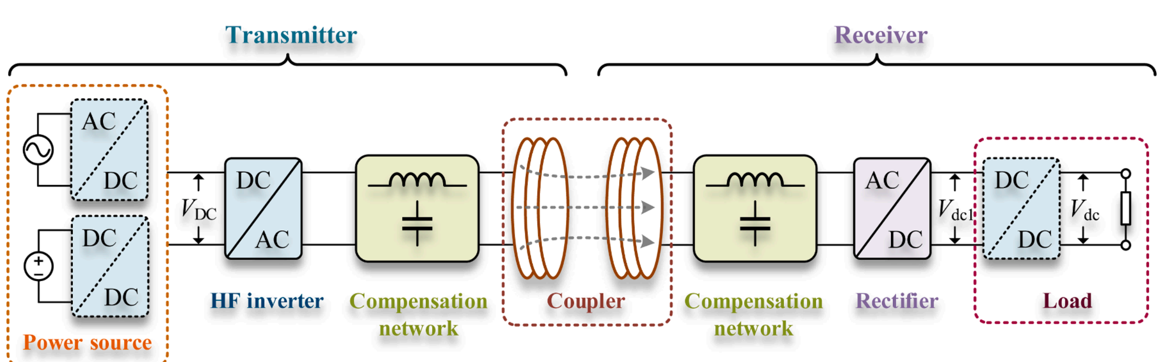


**Fig. 6.** Typical structure of WPT system.

additional core losses and can lead to variations in coil inductance when the coil's position changes, potentially resulting in system detuning. Moreover, reducing the transmission distance and optimizing coil design are constrained by practical application limits, as coil positioning and structure cannot be arbitrarily modified.

Following the methods discussed for increasing *k*-value and *Q*-value, extensive studies have investigated the structural and parameter design of couplers. Commonly used coil structures and their characteristics are summarized in Table 5.

The circular coil, the earliest coil structure utilized, boasts a simple design and requires less core material, achieving optimal coupling when aligned directly opposite each other (Bosshard et al., 2013). However, its limited flux path height restricts the energy transmission distance. Furthermore, it exhibits poor tolerance to misalignment: radial misalignment of 40% can reduce *k*-value to nearly zero (Budhia et al., 2011; Zaheer et al., 2014). Consequently, circular coils are typically used in static WPT systems that have simple structures and short transmission distances. To enhance misalignment tolerance, rectangular coil is a popular design choice, particularly in applications like EVs where lateral misalignment tolerance is crucial. This design increases the effective power transfer area of the coil, making it suitable for dynamic WPT (Luo and Wei, 2018; Chen et al., 2016b). Additionally, the flux path height of rectangular coil is twice that of circular coil, effectively increasing the transmission distance (Luo and Wei, 2018). Inspired by magnetic flux tubes, DD coil was proposed, featuring two coils connected in reverse series (Budhia et al., 2013). Unlike the vertical magnetic flux coupling of the previously mentioned two coil structures, the DD coil couples magnetic flux horizontally. Therefore, a DD coil used as a transmitter cannot transfer energy to a circular or rectangular coil, and vice versa (Bosshard et al., 2016). has compared the performance of rectangular and DD coils, concluding that DD coil has slightly lower transmission efficiency at the same power density, primarily due to higher core losses caused by increased magnetic flux density within the core. However, the DD coil reduces stray magnetic fields by half compared to rectangular coil, significantly enhancing the safety of WPT, especially in high-power applications. Yet, due to its horizontal flux coupling, the DD coil's lateral misalignment tolerance is limited. To address this issue, (Budhia et al., 2013) has proposed the addition of an orthogonal coil between the two original DD coils, thereby forming what is termed DDQ coil. The DDQ coil can couple magnetic flux both vertically and horizontally, greatly improving its misalignment tolerance. However, this new coil structure requires an additional HF inverter to drive the orthogonal coil, increasing both cost and complexity.

The analysis above clearly demonstrates that in coil design, it is crucial to not only maximize coupling coefficient *k* and quality factor *Q* but also to account for misalignment tolerance to enhance the stability of WPT.

### 3.1.2. Compensation network

The coupler in WPT systems functions similarly to a transformer. However, due to the loose coupling between the two coils, there is a large leakage inductance, which makes the use of compensation networks on both sides necessary. These compensation networks are tuned such that both the transmitter and the receiver can operate near the resonant frequency of the system, compensating for the reactive power caused by leakage inductance. Table 6 summarizes the structures and

**Table 5**
Structures and characteristics of commonly used couplers.

| Coil design | Structure | Direction of flux coupling | Misalignment Tolerance (lateral) | Flux path height |
|---|---|---|---|---|
| **Circular** | 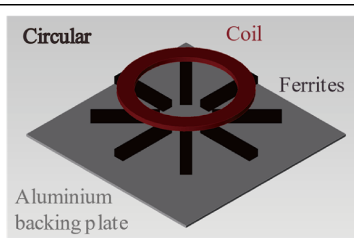 | Vertical | Null at 40% of diameter | 1/4 of coil diameter |
| **Rectangular** | 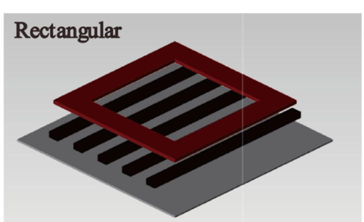 | Vertical | Better than circular coil | 1/4 of coil length |
| **DD** | 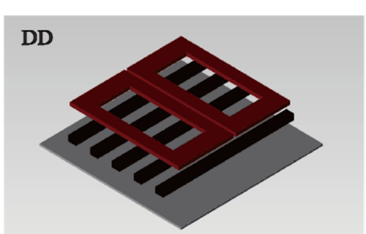 | Horizontal | Null at 34% of length | 1/2 of coil length |
| **DDQ** | 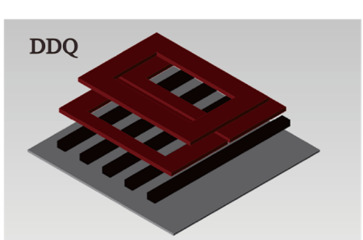 | Horizontal and vertical | Null at 95% of length | 1/2 of coil length |

**Table 6**
Structures and characteristics of commonly used compensation networks.

| Compensation network | Basic | | | |
|---|---|---|---|---|
| | **S-S** | **S-P** | **P-S** | **P-P** |
| **Structure** | 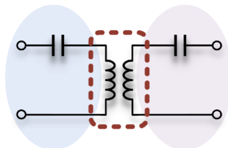 | 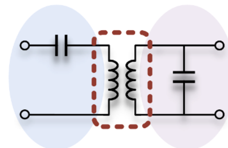 | 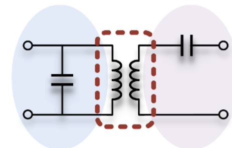 | 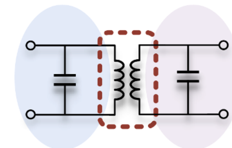 |
| **Output type** | Constant current | Constant voltage | Constant current | Constant voltage |
| **Parameter-dependent property** | Independent | Dependent on mutual inductance | Dependent on mutual inductance & load | Dependent on mutual inductance & load |
| **Sensitivity of Efficiency to load** | High | High | High | High |
| **Compensation network** | **High order** | | | |
| | **LCC-S** | | **LCC-LCC** | |
| **Structure** | 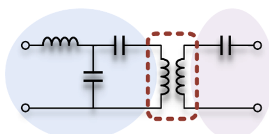 | | 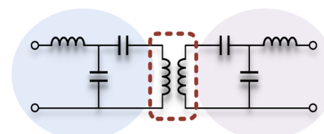 | |
| **Output type** | Constant voltage | | Constant current | |
| **Parameter-dependent property** | Independent | | Independent | |
| **Sensitivity of Efficiency to load** | Low | | Low | |

characteristics of frequently used compensation networks (Cota et al., 2019; Zhang et al., 2018, 2014; Mai et al., 2017; Huang et al., 2024). The four basic types of compensation network configurations are SS, PP, SP, and PS. These configurations are noted for their simplicity: SS and PS networks typically output a constant current, while PP and SP networks provide a constant voltage output. However, apart from the SS compensation network, the parameters of the other networks are influenced by the mutual inductance between coupling coils or by the load. This susceptibility can result in detuning when either the load or the mutual inductance changes. From a cost-effectiveness perspective, the SS network is also the most advantageous for high-power WPT systems among the basic compensation topologies (Sallán et al., 2009). However, it is not suitable for dynamic WPT due to its high sensitivity to changes in mutual inductance and load. Given the limitations of these four basic networks, higher order compensation topology compensation networks have been developed. The LCC-S and LCC-LCC configurations depicted in Table 6 are exemplary, offering better load dynamic characteristics and additional tuning flexibility compared to the four basic networks. However, these advanced configurations also increase design complexity and introduce additional losses. Therefore, it is crucial to select the appropriate compensation network based on specific application requirements.

### 3.1.3. Power converter

In WPT systems, the power source can be either a low frequency (LF) AC source, such as the utility grid charging EVs, or a DC source, such as energy trading between EVs (Mi et al., 2016; Patil et al., 2018). To enhance the quality factor of the coupler, it is necessary to convert the LF AC or DC from the power source side into HF AC through a power converter and inject it into the coupler. For most WPT systems, this conversion typically requires a two-stage process (Song et al., 2020). Initially, the LF AC source and DC source are connected to a voltage-stabilized DC bus via an AC/DC converter and a DC/DC converter, respectively. Subsequently, HF AC is generated from the DC bus through an HF DC/AC converter, which then powers the transmitter coil. Typically, the AC/DC or DC/AC converters employ an H-bridge structure with two switching components on each bridge. In this configuration, the ends of each bridge are connected to the DC side, and the midpoint is connected to the AC side (Ning et al., 2013). Switching components commonly used include metal-oxide-semiconductor field-effect transistors (MOSFETs) or insulated gate bipolar transistors (IGBTs). However, due to the limited switching frequency of IGBTs, they are generally used only in LF converters. To further enhance overall system performance, various converter structures have been developed with the goal of optimizing conversion efficiency and elevating both voltage and power levels (Wang et al., 2019; Baros et al., 2017; Malinowski et al., 2010; Liu et al., 2022b; Nguyen et al., 2014; Li et al., 2023). Moreover, due to the high switching frequency of the HF DC/AC converter, efforts must be made to achieve soft-switching to reduce switching losses (Li et al., 2021).

On the receiver side, the HF AC received is converted into DC through rectification and subsequent filtering to supply power to the load. In scenarios where ripple requirements are not significant and energy transfer is unidirectional, a diode bridge rectifier combined with a capacitor for filtering is typically employed (Li and Mi, 2015). However, to achieve bidirectional WPT, the rectifier must be configured as an HF converter (Pasupuleti et al., 2023).

## 3.2. HTS-WPT technology

So far, Cu Litz wire is commonly used as the coil material in WPT systems due to its low cost and minimal susceptibility to skin and proximity effects. However, due to the inherent properties of Cu, there is a limit to the coupling coefficient at a given operating frequency, which constrains the transmission efficiency of WPT systems. In contrast, superconducting materials exhibit virtually zero resistance below transition temperatures and can support current densities ranging from $10^3$ to $10^5$ A/mm$^2$, far surpassing the typical current density of 5–10 A/mm$^2$ in Cu, Theoretically, this allows for the production of coils with a smaller size yet higher *Q*-value, significantly enhancing the transmission efficiency and power density of WPT systems. Considering the complexity and costs associated with the cooling systems required for superconducting technology, HTS materials are favored over LTS materials because they can achieve superconductivity at the temperature of $LN_2$. Research on HTS-WPT systems is still in its early stages, with some researchers exploring various power levels and system configurations in

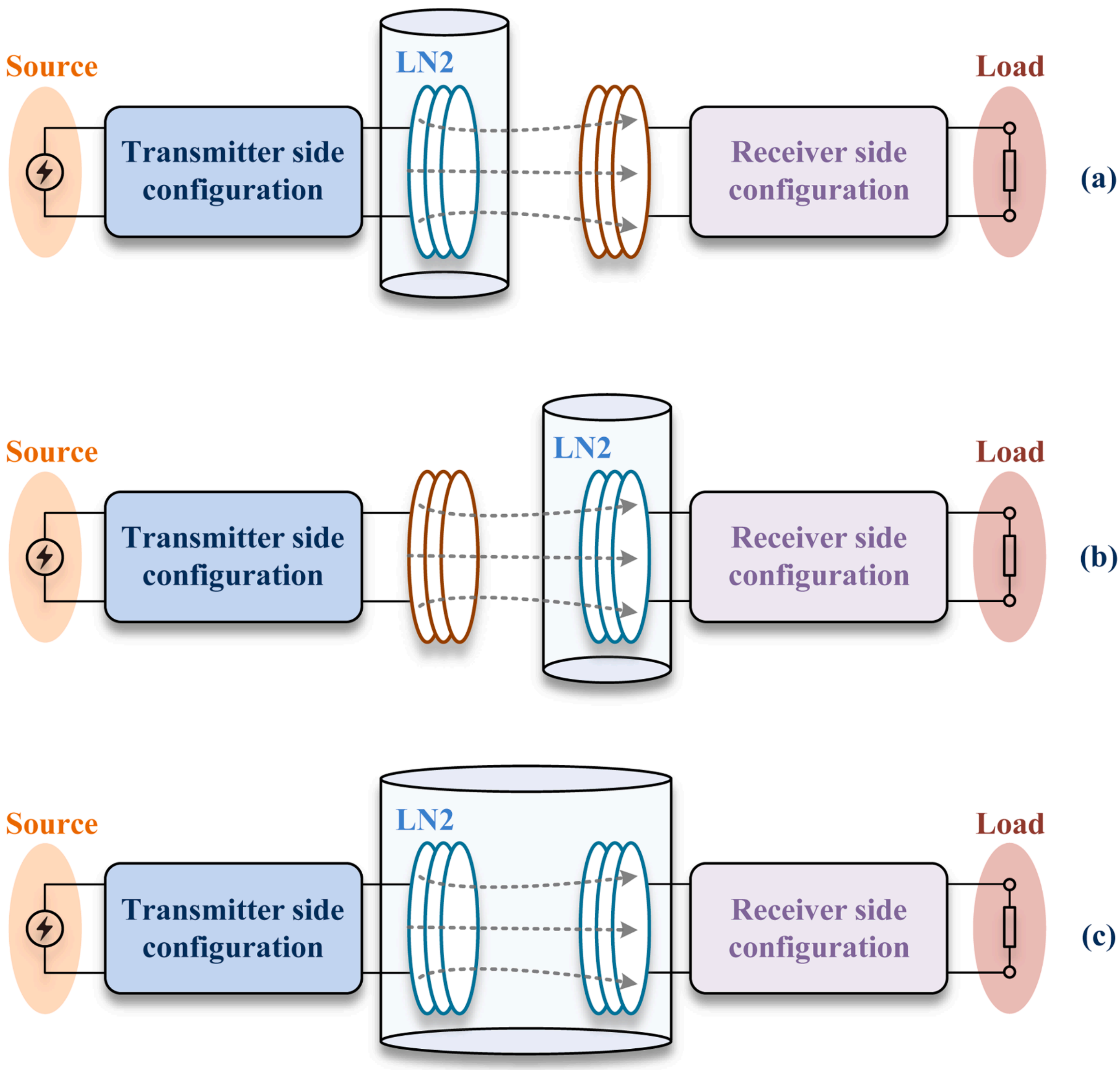


**Fig. 7.** Typical structures of three types of HTS-WPT systems. (a) Transmitter-side superconducting HTS-WPT systems. (b) Receiver-side superconducting HTS-WPT systems. (c) Dual-side superconducting HTS-WPT systems.

laboratory settings. Depending on their system structures, HTS-WPT systems can be categorized into three types: transmitter-side superconducting, receiver-side superconducting, or dual-side superconducting, as illustrated in.

### 3.2.1. *Receiver-side superconducting HTS-WPT system*

Kim et al., (2012), (2013) were the first to propose the use of HTS coils as replacements for Cu couplers in WPT systems, with configurations set to receiver-side superconducting and experiments conducted at a radio frequency of 13.56 MHz (Kim et al., 2012). evaluated the transmission efficiency using HTS versus Cu materials for the receiving coil at a power level of 200 W, and observed notable enhancements in efficiency with HTS coils (Kim et al., 2013). examined a multi-coil resonant system, illustrated in (a), consisting of four coils tuned to the same resonant frequency, including the power coil, transmitter coil, receiver coil, and load coil. In this setup, the receiver coil and load coil were fabricated from HTS materials, while the power coil and transmitter coil were made of Cu. The study investigated the transmission characteristics over a 1.1 m distance between the transmitter and receiver coils. The findings highlighted that at a 0.3 m distance from the Cu transmitter coil to the HTS receiver coil, the peak transmission efficiencies for current and voltage exceeded 50% and 70%, respectively. However, the absence of a comparative analysis with conventional Cu coils in the study did not highlight the system's performance superiority. Additionally, both studies indicated that using HTS coils with a higher *Q*-value as receiving coils appears to be more advantageous than using them as transmitting coils.

Following these two studies, (Do Chung et al., 2019; Qian et al., 2019; Do Chung et al., 2017) conducted extensive theoretical and experimental research on receiver-side superconducting HTS-WPT systems. The system configurations and parameters for these studies are summarized in Table 7 (Do Chung et al., 2019). compared the system performance using Cu coils versus HTS coils as receiving coils at resonance frequencies of 100 kHz and 370 kHz. The experimental results indicated that transmission efficiency significantly improves at 370 kHz. Furthermore, a comparison at $LN_2$ temperatures showed that, even though the resistance of the Cu coil decreases at low temperatures, its transmission efficiency remained lower than that of the HTS coil. Additionally, due to higher thermal losses, the Cu coil consumed more $LN_2$ (Qian et al., 2019). integrated the receiving coil with a cryogenic rectifier to collectively power a superconducting magnet, thereby eliminating interface losses from the cryogenic vessel and room temperature. However, the experimental setup in this study exhibited low efficiency, which the researchers attributed to the long transmission

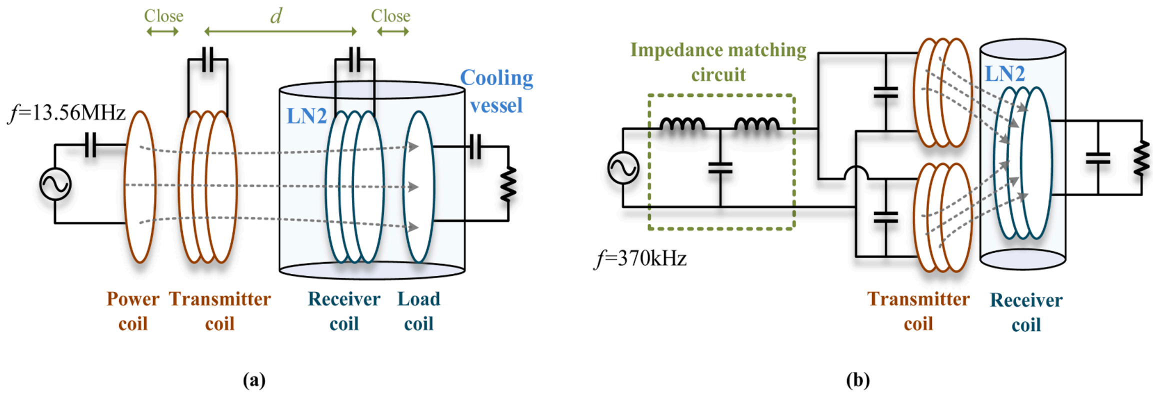


**Fig. 8.** Experimental setup of receiver-side superconducting HTS-WPT systems. (a) Topology (Kim et al., 2013). (b) Topology (Do Chung et al., 2017).

**Table 7**
System configurations and parameters of reported HTS-WPT studies.

| System configuration | Reference | Year of publication | Power level | Peak efficiency (Transmission efficiency/ System efficiency) | Coil diameter (Transmitter/ Receiver) | Transmission distance | Q-value of HTS coil | Resonant frequency |
|---|---|---|---|---|---|---|---|---|
| Receiver-side superconducting | (Kim et al., 2012) | 2012 | 200 W | –/– | –/0.28 m | 0.5 m | ~934 | 13.56 MHz |
| | (Kim et al., 2013) | 2013 | – | –/– | 0.33 m/0.3 m | 0.3–1.1 m | – | 13.56 MHz |
| | (Do Chung et al., 2019) | 2019 | 250 W | ~60%/– (100 kHz) ~70%/– (370 kHz) | 0.3 m×0.8 m/ 0.3 m×0.4 m (rectangular) | 0.1–0.2 m | 200/260 | 100/ 370 kHz |
| | (Qian et al., 2019) | 2019 | – | – | 0.1 m/0.1 m | 0.03–0.1 m | – | 80–90 kHz |
| | (Do Chung et al., 2017) | 2017 | 300 W | <70%/– | 0.3 m/0.3 m | 0.15 m | 200–350 | 370 kHz |
| Transmitter-side superconducting | (Do Chung et al., 2013) | 2014 | <50 W | –/– | 0.28 m/0.3 m | 0.3–1 m | – | 370 kHz |
| | (Do Chung et al., 2014) | 2015 | 500 W | <60%/– | 0.3 m/0.3 m | 0.3 m | 200 | 370 kHz |
| | (Do Chung et al., 2016) | 2016 | 600 W | 70%~80%/– | 0.3 m/0.3 m | 0.25 m | 200 | 370 kHz |
| | (Okeda et al., 2022) | 2022 | – | <80%/– | 0.235 m/0.248 m | 0.65 m | 14100 | 9 MHz |
| | (Sekiya et al., 2023) | 2023 | – | <50%/– | 0.235 m/0.01 m | 0.15 m | 13102 | 9 MHz |
| | (Zuo et al., 2014) | 2015 | 200 W | >90%/~80% | 0.315 m/0.315 m | 0.1 m | ~664 | 50 kHz |
| | (Inoue et al., 2024) | 2024 | 1 kW | –/>98% | 0.41 m/0.4 m | 0.05 m | 2884 | 4.8 kHz |
| | (Inoue et al., 2023a) * | 2023 | 100 kW | >98%/91.4% | 0.5 m/0.5 m | 0.1 m | 1318 | 4.5 kHz |
| Dual-side superconducting | (Machura et al., 2020) * | 2020 | <150 kW | 94.6%/62.17% | 0.125 m/0.125 m | 0.01–0.125 m | – | 85 kHz |
| | (Sekiya and Sawada, 2023) | 2023 | 1 mW | 90%/– | 0.25 m/0.25 m | 0.8 m | 19617 | 8.06 MHz |
| | (Utschick et al., 2021) | 2021 | 6 kW | 97%/– | 0.22 m/0.22 m | –($k$ = ~0.5) | <100 | 110 kHz |
| | (Inoue et al., 2022a,b,c) * | 2022 | 200–600 kW | –/92.6% | 0.8 m/0.8 m | 0.12 m | – | 10 kHz |
| | (Inoue et al., 2019) * | 2019 | 38.7 kW | >90%/– | 0.8 m×0.8 m/ 0.8 m×0.8 m (rectangular) | 0.075 m | – | 0.8/4.3 kHz |
| | (Inoue et al., 2021)* | 2021 | 20–100 kW | –/>87% | 0.8 m/0.8 m | 0.08 m | – | 2 kHz |
| | (Inoue et al., 2022a,b) | 2023 | 1 kW | 99%/96% | 0.4 m/0.4 m | 0.04 m | >1000 | 0.92 kHz |
| | (Inoue et al., 2023b) * | 2023 | 250 kW | –/>90% | ~0.8 m×1 m/ 0.8 m×1 m (rectangular) | 0.12 m | ~1000 | 1–5 kHz |

References marked with * are without experimental set-ups.
– indicates that it is not mentioned in references.

distance and higher optimal operating frequency. Thus, this system requires further investigation (Do Chung et al., 2017). developed a receiver-side superconducting HTS-WPT system with multiple transmitter coils and one receiver coil, as shown in (b), achieving 300 W power transmission at 370 kHz. Although the experimental results demonstrated that the HTS receiving coil improved efficiency by approximately 20% compared to the Cu coil at cryogenic temperatures and reduced $LN_2$ consumption by about 30%, the peak system efficiency was still below 70%, affecting the demonstration of research outcomes.

### 3.2.2. Transmitter-side superconducting HTS-WPT system

Contrary to the findings of (Kim et al., 2012, 2013), (Zhang et al., 2013) demonstrated that using HTS coils as transmitter coils resulted in better system performance than using them as receiver coils in HTS-WPT systems. This conclusion was drawn by comparing the performance of transmitter-side superconducting, receiver-side superconducting, and dual-side superconducting HTS-WPT systems at a resonance frequency of 3 kHz and a transmission power of 11 W (Yu et al., 2018). further investigated this asymmetry through experiments at resonance frequencies of 3 kHz and 20 kHz. The theoretical analysis and experimental results revealed that the asymmetry originated from the different resistances of HTS and Cu coils. The study suggested that optimizing the load could eliminate the effects of this asymmetry (Do Chung et al., 2013, 2014, 2016; Okeda et al., 2022; Sekiya et al., 2023; Zuo et al., 2014; Inoue et al., 2024, 2023a). conducted theoretical and experimental research on transmitter-side superconducting HTS-WPT systems, with the system configurations and parameters summarized in Table 7. In (Do Chung et al., 2013), researchers investigated the effects of replacing Cu coil at the transmitter side with an HTS coil at a resonant frequency of 370 kHz, and further increased the transmission distance by adding a resonant coil to the experimental platform. The results showed that as the transmission distance $d$ increased from 0.3 m to 1 m, the HTS-WPT system transmitted 11% ($d = 0.7$ m) and 52% ($d = 0.3$ m) more power compared to the conventional WPT system (Do Chung et al., 2014, 2016). conducted by the same principal researcher focused on the transmitter-side superconducting HTS-WPT system. Both studies had a coil diameter of 0.3 m and a resonant frequency of 370 kHz, with transmission distances of 0.3 m and 0.25 m, respectively. The difference lies in the experimental setup; (Do Chung et al., 2016) added an HTS resonant coil between the HTS coil and the Cu coil, enhancing the transmission efficiency compared to the setup in (Do Chung et al., 2014). Moreover, (Okeda et al., 2022; Sekiya et al., 2023) utilized HTS coils with a $Q$-value of over 10,000 to design WPT systems. In (Okeda et al., 2022), the HTS-WPT system maintained nearly 80% transmission efficiency at a distance of 0.6 m, significantly higher than the approximately 50% efficiency of conventional WPT systems (Sekiya et al., 2023). details the design of a WPT device for biomedical capsule endoscopy, maintaining a 50% charging efficiency even when a liquid phantom is present in the transmission path (Zuo et al., 2014). constructed an experimental platform for an HTS-WPT system with SS compensation network, transmitting power of 200 W at a resonance frequency of 50 kHz. The study investigated its output characteristics and found them to be consistent with the general trends of conventional WPT systems. Unlike the studies at resonance frequencies above 370 kHz, this platform achieved a transmission efficiency above 90%, with an overall efficiency, including the cooling system, of approximately 80% (Inoue et al., 2024). and (Inoue et al., 2023a) respectively conducted simulation and experimental studies on transmitter-side superconducting HTS-WPT systems at even lower frequencies (Inoue et al., 2024). focused on a LF, high-power HTS-WPT system, establishing a 1 kW experimental platform that achieved a system efficiency of over 98% at a resonance frequency of 4.8 kHz. The study highlighted the need to suppress conductor resistance losses and capacitor losses, in addition to AC losses, in high-power HTS-WPT systems (Inoue et al., 2023a). performed a simulation analysis of an HTS-WPT system with a resonance frequency of 4.5 kHz and power of 100 kW, achieving a transmission efficiency of 98% and a system efficiency of 91.4%. The study noted that HTS coils with high $Q$-value are more suitable for LF WPT systems, and increasing the frequency can reduce the mutual inductance of the coupler, thereby decreasing the size and weight of the coils.

### 3.2.3. Dual-side superconducting HTS-WPT system

It is reasonable to infer that dual-side superconducting HTS-WPT systems exhibit higher $Q$-value in the coupler, resulting in superior transmission performance compared to the HTS-WPT systems employing HTS coil on only one side (Machura et al., 2020; Utschick et al., 2021; Inoue et al., 2022a,b,c, 2019, 2021, 2023b). focus on dual-side superconducting HTS-WPT systems, with the relevant system configurations and parameters summarized in Table 7 (Machura et al., 2020). analyzed an HTS-WPT system with a resonance frequency of 85 kHz for WPT system of EVs based on simulations. The peak transmission efficiency and system efficiency were 94.6% and 62.17%, respectively. These results indicate that using conventional HTS coated conductors (CC) in HF WPT systems is impractical. The significant AC losses generated by HTS coils lead to excessive cooling power requirements, ultimately reducing overall system efficiency (Sekiya and Sawada, 2023). reported a pair of HTS coils that achieved a $Q$-value close to 20, 000. These coils were comprised of two REBCO CC tapes connected together using PTFE film strips, and by reducing the thickness of the Ag protection layer, skin effects were suppressed. This led to lower AC losses and thereby enhanced coil performance. When these coils were used in a WPT system with a resonant frequency of 8 MHz, they achieved a greater transmission distance compared to similar systems using Cu coils. At a transmission distance of 80 cm, this system achieved a measured transmission efficiency of 90%, while the efficiency of the conventional WPT system was only 28%. Furthermore, as previously analyzed, the AC losses of HTS coils increase with both current magnitude and frequency. Therefore, to achieve high efficiency in high power transmission applications, it is necessary to lower the resonance frequency (Inoue et al., 2022a,b,c, 2019, 2021, 2023b). investigated LF HTS-WPT systems through simulation analyses and experimental validations. These studies consistently demonstrated that LF, high-power HTS-WPT systems exhibit significantly higher transmission and system efficiencies compared to conventional WPT systems, underscoring the potential of HTS-WPT technology. Among these studies, the maximum transmission power achieved in simulated HTS-WPT systems was 600 kW, with system efficiencies reaching up to 92.6% (Inoue et al., 2022a,b,c). In practical HTS-WPT experimental setups, the highest transmission power achieved was 6 kW, with a transmission efficiency of 97% (Utschick et al., 2021). The power density related to coil area, weight, and volume for this system were 1.59 kW/$dm^2$, 5.71 kW/kg, and 7.95 kW/$dm^3$, respectively. These values surpass the power density of the most advanced conventional WPT systems currently available. However, this comparison only considers the power density of the coils. When taking into account the overall power density, including the cooling vessel, the advantages of HTS-WPT systems may be diminished.

In addition to the three typical HTS-WPT system configurations

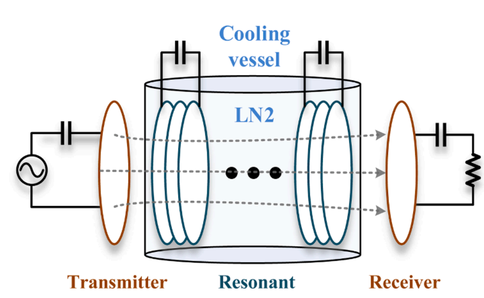


**Fig. 9.** Typical structures of resonant coil superconducting HTS-WPT systems.

mentioned above, (Li et al., 2019) and (Oshimoto et al., 2023) investigated resonant coil superconducting configurations, as shown in, through simulations and experimental studies, respectively. This configuration enhances system efficiency by incorporating HTS resonant coils between conventional Cu transmitter and receiver coils in WPT systems. Both experimental and simulation results demonstrated that HTS resonant coils significantly outperform Cu resonant coils.

These studies above encompass a variety of system configurations, power levels, coil structures, and transmission distances in HTS-WPT systems. A common finding across these studies is that HTS coils can achieve a *Q*-value significantly higher than that of Cu coils with identical structural parameters. Consequently, HTS-WPT systems exhibit superior transmission performance compared to conventional WPT systems based on Cu coils.

### *3.3. System applications*

Due to the higher *Q*-value of HTS coils compared to Cu coils, researchers have explored replacing Cu coils in conventional WPT systems with HTS coils to achieve better transmission performance. These studies span a range of applications, from a few watts in implanted medical devices (Sekiya et al., 2023) to several tens of kilowatts in high-power EV WPT systems (Do Chung et al., 2014, 2016; Inoue et al., 2024, 2023a). However, unlike Cu coils, HTS coils need to operate at $LN_2$ temperatures or even lower, and the AC losses in HTS coils during operation lead to significant increases in cooling power requirements. Additionally, the installation of cooling apparatus requires extra space and adds costs, which undermines the HTS coils' advantage in terms of power density.

Advancements in cryogenic technology or alternative cooling methods can alleviate the challenges associated with cryogenic operations. There are several approaches: firstly, the development of more advanced cooling technologies, such as pulse tube refrigerators, which can substantially reduce the energy required to maintain cryogenic conditions (Yazdani-Asrami et al., 2022). Secondly, innovations in coolants represent a significant breakthrough in technology. Lastly, in appropriate scenarios, the use of alternative energies, such as energy recovery systems that utilize waste heat to power cooling systems, can enhance the overall energy efficiency of the systems. However, the effectiveness of these cryogenic technologies or alternative cooling methods in terms of cooling performance and cost-efficiency remains to be further verified. Regardless of the progress in these cooling methods, the need for cooling equipment continues to pose a significant challenge to HTS-WPT systems.

Therefore, to fully leverage the advantages of HTS-WPT systems, it is recommended to use HTS-WPT technology in applications where cryogenic environments are more readily achievable, thereby reducing the costs associated with cooling apparatus. Compared to conventional applications like EVs, the recommended scenarios for HTS-WPT systems include settings where HTS materials are already in use and require cryogenic operational environments. By integrating HTS-WPT systems into such scenarios, one can not only enhance system performance but also capitalize on existing cooling infrastructure. This synergistic use of existing resources allows HTS-WPT systems to fully realize their transmission performance benefits, making them more viable and effective in these applications.

#### *3.3.1. Power supply for HTS magnets*

HTS magnets, with their zero-resistance characteristics, high current-carrying capacity, and excellent magnetic field performance, have demonstrated promising applications in MRI, maglev trains, and high-field laboratory magnets (Weijers et al., 2010; Iwasa, 2003). However, due to the flux creep in HTS materials under external magnetic fields, the current in HTS magnets inevitably decays, necessitating an external power supply to maintain the current level (Beasley et al., 1969). The conventional method involves the use of current leads, with one end connected to the power supply at ambient temperature and the other end connected to the HTS magnet at cryogenic temperatures. This setup, however, results in significant thermal leakage at the interface of the current leads and the cryogenic vessel, increasing cooling costs and posing a risk of quenching the HTS magnets. To address this issue, employing HTS-WPT system to power superconducting magnets is an ideal solution (Hwang and Jang, 2022; Zhou et al., 2020). The WPT system establishes magnetic coupling between the power supply and the HTS magnet, thereby eliminating physical interfaces and thereby reducing thermal losses. Additionally, since the HTS magnet is situated in a cryogenic environment, using HTS coil on the receiver side can significantly enhance transmission performance while reducing the additional costs associated with cooling apparatus. Fig. 10 illustrates the schematic diagram of this system (Qian et al., 2019).

#### *3.3.2. HTS cable termination*

HTS cables, with higher capacity and lower losses compared to conventional cables, have increasingly been applied in recent years (Endo et al., 2022; Fetisov et al., 2021). Currently, there is a mechanical connection between the HTS cables and conventional cables, as shown in Fig. 11(a). However, thermal intrusion from the ambient temperature section can lead to mechanical degradation, the contact resistance between HTS and conventional cables can cause heat generation, both of which can result in poor contact and increased cooling losses (Masuda et al., 2007). The HTS-WPT system is a promising solution to these issues, as it physically separates the HTS cable section from the ambient temperature section where the conventional coils are located, as shown in Fig. 11(b) (Inoue et al., 2022b). In this HTS-WPT system, the gap between the transmitter coil and the receiver coil is minimal, ensuring excellent transmission performance. Furthermore, the HTS cable side provides the necessary cryogenic environment for the HTS coil.

#### *3.3.3. Power supply on spacecrafts*

Certain specialized systems on spacecraft, such as electronic systems and superconducting machines, require operation in cryogenic environments (Rajashekara and Akin, 2013). However, most current power supplies and power electronic circuits function reliably only at room temperature. Typically, the design involves isolating the power electronic circuits from the cryogenic environment and supplying power to the low-temperature systems via current leads (Bourne et al., 2008). As previously mentioned, this design results in significant thermal losses at the interface between the cryogenic and room temperature environments, thereby reducing system efficiency. The adoption of HTS-WPT systems can ensure the integrity of the cryogenic environment, as shown in Fig. 12. Additionally, recent studies have shown that some switching components can operate normally and even perform better at low temperatures, suggesting that power electronic circuits may have superior performance in cryogenic conditions compared to those at room temperature (Garrett et al., 2006; Elbuluk and Hammoud, 2005). This implies that future spacecraft could potentially operate entirely in cryogenic environments, eliminating the need for additional thermal insulation layers and simplifying system design. In such scenarios, an HTS-WPT system capable of transmitting energy from the external room-temperature environment to the sealed cryogenic environment within the spacecraft could be indispensable.

## 4. Discussion

### *4.1. Developing trend*

In the rapid advancement of HTS-WPT technology, identifying and addressing key technical challenges is crucial. The following sections will delve into these research directions and their potential developing trends.

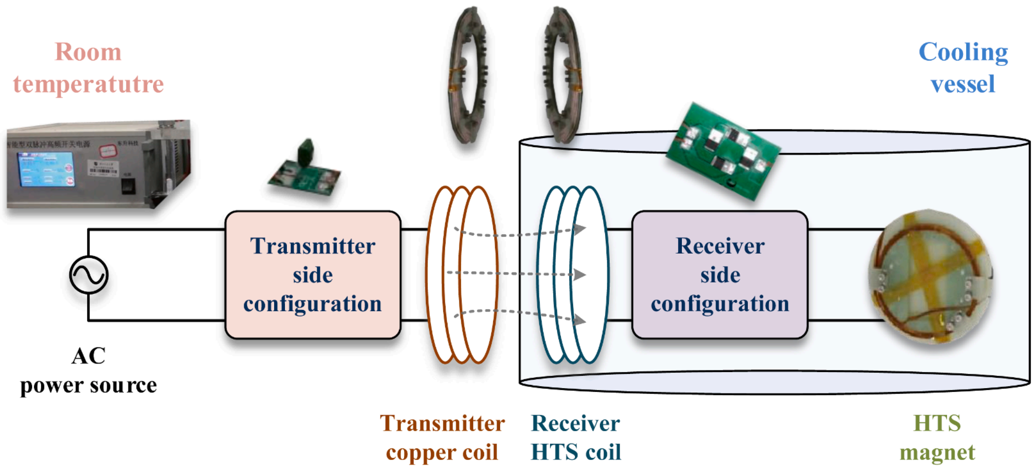


**Fig. 10.** HTS-WPT system for HTS magnet power supply (Qian et al., 2019).

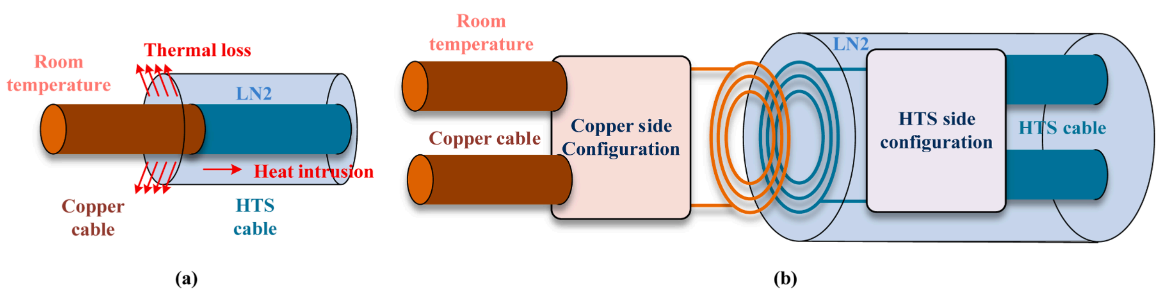


**Fig. 11.** Schematic diagram of HTS cable termination. (a) Conventional cable termination. (b) HTS-WPT cable termination.

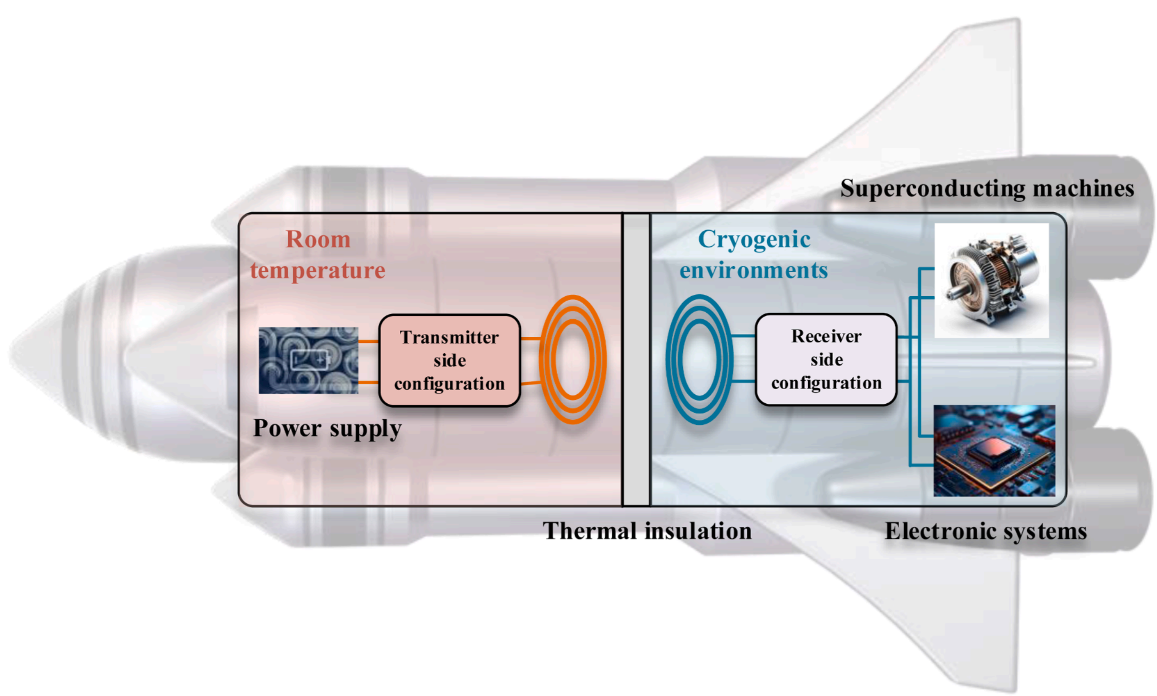


**Fig. 12.** Schematic diagram of HTS-WPT system for spacecraft power supply.

*4.1.1. Strategies to reduce AC losses*

HTS coils must operate in cryogenic environments to maintain high Q-values and high current density, necessitating additional cooling power to compensate for the heat generated by AC losses. Unlike conventional WPT systems, the overall losses in HTS-WPT systems include not only transmission losses but also the cooling power required to maintain the cryogenic environment. As a result, although HTS-WPT systems generally exhibit much higher transmission efficiency compared to conventional WPT systems, the overall efficiency improvement may not be as significant. Therefore, it is essential to reduce the AC losses in HTS-WPT systems and lower the required cooling power to further promote the application of HTS-WPT technology.

One mainstream approach is to reconsider the operating conditions of the system. In the early development of HTS-WPT systems, researchers initially focused on directly replacing Cu coils in conventional WPT systems with HTS coils. However, the experimental results were suboptimal. The primary reason is that conventional WPT systems, constrained by the material properties of Cu coils, require the selection of relatively high resonance frequencies to maximize the *Q*-value. At such high frequencies, the AC losses in HTS coils are substantial, which significantly increases the cooling power requirements and severely impacts system efficiency. As mentioned in Section 2, the AC losses in HTS materials are proportional to the frequency and magnitude of the current. To fully leverage the advantage of HTS coils' high critical current density, LF, high-capacity HTS-WPT systems have become a research focus. Fig. 13 illustrates the relationship between power levels and resonance frequencies of experimental setups reported in the references. It is evident that high-power HTS-WPT systems are trending towards LF. Currently, the highest power level reported for an HTS-WPT system is 6 kW with a system resonant frequency of 110 kHz (Utschick et al., 2021). However, the authors of this study have noted that while the experiments were conducted at higher frequencies, there is an anticipated improvement in efficiency and accessible power levels by reducing the resonant frequency to the lower frequency region (Machura and Li, 2021; Jang et al., 2024). have also proposed other promising methods to reduce AC losses (Machura and Li, 2021). have explored the application of flux diverters in HF HTS-WPT systems. AC losses are primarily caused by magnetic fluxes perpendicular to the tape surface (Li et al., 2016). In such cases, these fluxes are mainly around the edges of the HTS coils, and flux diverters can effectively divert these fluxes, thereby reducing the losses. Although flux diverters have been shown to effectively reduce AC losses at LF (~50 Hz), their effectiveness at HF (>10 kHz) has not been significant (Jang et al., 2024). has attempted to minimize AC losses and improve system efficiency by optimizing system parameters, including coil parameters (such as coil size and the number of turns) and circuit parameters (such as power supply voltage, resonant frequency, and load).

In conclusion, before HTS-WPT systems can be fully industrialized, research on methods to reduce AC losses in HTS coils and ensuring significant improvements in system efficiency will be the most critical steps.

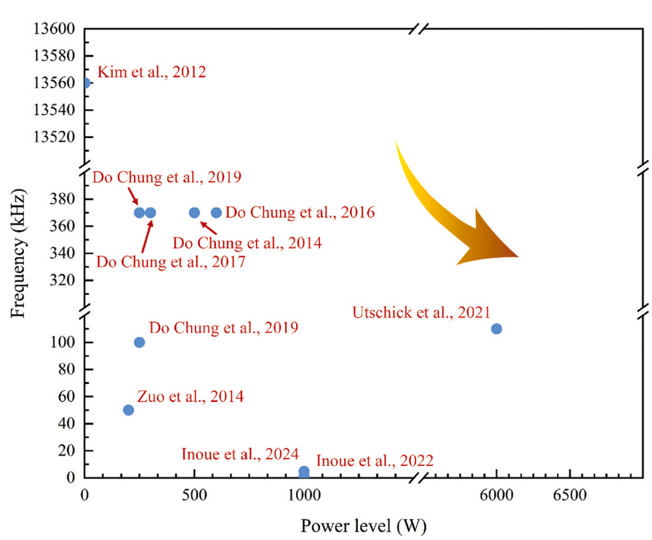


**Fig. 13.** Relationship between power levels and resonance frequencies of experimental setups reported in References.

### 4.1.2. *Advanced HTS coil materials for enhanced performance*

Considering cost and manufacturing constraints, current HTS-WPT systems typically use REBCO CC tapes or Bi-2223 Ag-sheathed tapes to fabricate HTS coils (Jeong et al., 2018). The detailed fabrication methods for both REBCO CC tapes and Bi-2223 Ag-sheathed tapes are elaborately described in (Yao and Ma, 2021). For Bi-2223 tapes, the PIT method is utilized, starting with mixed oxides and carbonates that are calcined to create precursors. These precursors are then packed into a metal sheath and mechanically deformed into tapes. Silver (Ag) or Ag alloy is employed as the sheath material instead of Cu and other metals due to its chemical compatibility with the precursor and its transparency to oxygen, which is crucial for facilitating the oxygen exchange necessary during heat treatment. For REBCO CC tapes, in addition to the PIT method, REBCO films are deposited on biaxially textured buffer layers that are coated onto a long, flexible, tape-like metal substrate. To enhance environmental protection and thermal stabilization, a thin layer of Ag a few micrometers thick and a thicker layer of Cu are applied over the conductor.

However, due to the skin effect, HF currents mainly flow through the Cu stabilizer in REBCO CC tapes and the silver sheath in Bi-2223 Ag-sheathed tapes, severely compromising the coil's *Q*-value (Machura et al., 2020; Yuan and Shen, 2004). To mitigate this issue, it is necessary to remove the outer Cu stabilizer and Ag sheath, but this renders the materials difficult to process further. Additionally, for REBCO CC tapes, removing the Cu stabilizer exposes the outermost Hastelloy substrate, which has low electrical conductivity, significantly increasing the conductive losses of the HTS coil.

Sekiya and Monjugawa (2017); Sekiya and Sawada (2023) have developed REBCO CC tapes suitable for radio frequency (MHz) WPT systems. A comparison between these advanced tapes and conventional REBCO CC tapes is shown in Fig. 14. These advanced tapes consist of two conventional REBCO CC tapes with the Cu stabilizer removed, allowing HF currents to flow within the REBCO layer, which significantly reduces coil losses. In terms of *Q*-value, coils fabricated from these advanced conductor tapes achieve a *Q*-value close to 20,000, which is more than 4.95 times that of conventional REBCO coils and 21.07 times that of Cu coils. However, research on HTS coil materials at LF (kHz) remains limited. Balancing the cost and performance of coils, and developing suitable HTS coils, is crucial for the broader application of HTS-WPT systems in the future.

### 4.1.3. *Component design for low-temperature operation*

In the typical application scenarios of HTS-WPT systems mentioned in Section 3, not only do HTS coils operate in cryogenic environments, but other modules, such as the compensation network and converters, also need to function under low-temperature conditions. However, significant temperature variations can markedly affect both their static and dynamic characteristics. Besides HTS coils, HTS-WPT systems include the following components: 1) switching components, including diodes and active switches such as MOSFETs; 2) passive components, including inductors, capacitors, and resistors in power or control circuits; and 3) integrated circuits, including control circuits and gate drive circuits. Investigating the operational characteristics of these components at low temperatures is crucial for ensuring the safe and reliable operation of HTS-WPT systems.

Some literature has studied the performance of conventional switching components, passive components, and integrated circuits at low temperatures, providing a certain understanding of their low-temperature characteristics. However, to fully leverage the advantages of HTS-WPT systems, it is necessary to further design components specifically for low-temperature operation, such as the HTS capacitors mentioned in Section 2.

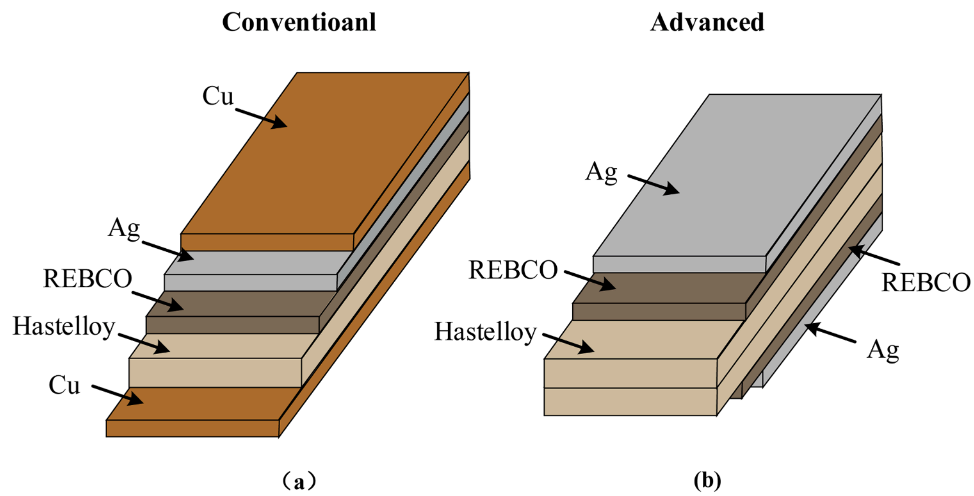


**Fig. 14.** Structures of REBCO CC tape. (a) Conventional REBCO CC tape. (b) Advanced REBCO CC tape in (Sekiya and Monjugawa, 2017).

#### 4.1.4. Other auxiliary functions

Currently, research on HTS-WPT systems primarily focuses on one transmitter coil to one receiver coil static energy transfer. However, similar to conventional WPT systems, HTS-WPT systems need to incorporate auxiliary functions to ensure stable and reliable energy transfer across different application scenarios.

Inoue et al., (2023b); Tian et al., (2022) have investigated methods to enhance the misalignment tolerance of HTS-WPT systems (Inoue et al., 2023b). examines the impact of coil structure on the misalignment tolerance of HTS-WPT systems. The study finds that compared to using circular HTS coils, employing non-circular HTS coils results in more robust received power and system efficiency against misalignment. It is recommended to use long rectangular or elliptical coils in the longitudinal direction of the track in WPT systems with significant lateral misalignment to improve system efficiency (Tian et al., 2022). explores an optimal current algorithm based on energy beam-forming technology, where optimal current vectors are obtained by utilizing information on different input impedance characteristics of the transmitting coils, thus achieving maximum output power tracking for various receiver positions.

Do Chung and Lee (2023) investigates a multi-frequency HTS-WPT system that employs two power sources of different frequencies to supply power to the load through two physically independent HTS-WPT systems, as illustrated in Fig. 15. The study concludes that better transmission performance is achieved when the frequency difference between the two power sources is large, due to reduced electromagnetic interference. Additionally, with shielding between the two HTS-WPT systems, the electric field energy between the transmitting and receiving coils is stronger.

Compared to conventional WPT systems, research on these auxiliary functions in HTS-WPT systems is still in its infancy and remains sparse and incomplete. As HTS-WPT technology continues to mature, more detailed investigations into these auxiliary functions will be necessary.

### 4.2. Limitation

So far, the primary limitation in the development of HTS-WPT systems is the need for additional cooling apparatus to maintain the cryogenic environment. On one hand, this increases losses and lowers the overall system efficiency. On the other hand, the installation of cooling equipment reduces the system’s power density and adds to its complexity. These factors offset the potential performance improvements that HTS coils could bring to WPT systems.

Another limitation is the current manufacturing level of HTS materials. As mentioned earlier, commonly used superconducting tapes have Cu stabilizers or Ag sheaths, which are significantly affected by the skin effect at high frequencies. Furthermore, studies have shown that excessive bending of these superconducting tapes can result in the loss of

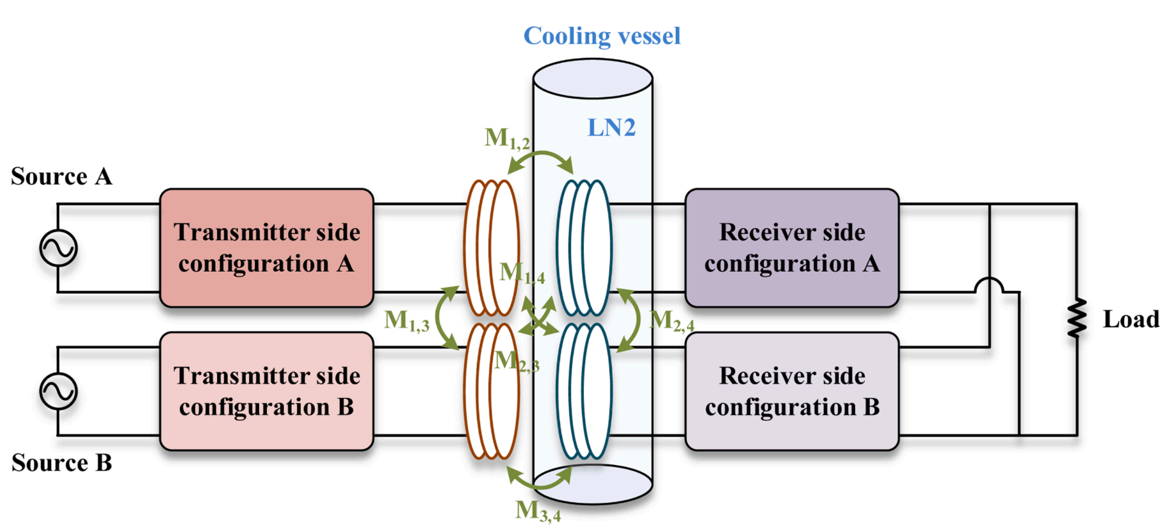


**Fig. 15.** Schematic diagram of the multi-frequency HTS-WPT system in (Tian et al., 2022).

superconductivity, further complicating the fabrication of HTS coils (Jeong et al., 2015; Yoo et al., 2018).

Finally, the characteristics of the various components in the WPT system may change at low temperatures, thus affecting system reliability. In order to ensure better and stable system performance of the HTS-WPT system at low temperatures, it is necessary to investigate and verify the system performance in detail.

In conclusion, while HTS-WPT systems hold significant promise for enhancing WPT performance, several key challenges such as the necessity of a complex cooling system, limitations in the current state of HTS material manufacturing, and changes in component properties at low-temperatures need to be tackled. Only by addressing these issues can the full potential of HTS-WPT systems be realised, paving the way for more efficient and reliable WPT technologies.

## 5. Conclusions

This article provides a comprehensive and in-depth review of the key topics, major characteristics, recent technological breakthroughs, and potential applications of HTS-WPT technology. The main contributions are summarized below:

(1) The article provides a detailed classification of HTS materials, highlighting critical parameters including transition temperature, critical magnetic field strength, and critical current density. By leveraging the higher maximum current density and lower losses of HTS materials, it is feasible to fabricate circuit components such as HTS inductors and capacitors, significantly enhancing the efficiency and power density of WPT systems.
(2) The article systematically reviews the parameters and configurations of current HTS-WPT systems, analyzing the benefits and limitations of HTS technology. It points out that replacing Cu coils with HTS coils in conventional WPT systems has the potential to significantly enhance the transmission performance. Notably, in applications scenarios where cryogenic environments already exist, HTS-WPT systems can fully exploit their advantages, resulting in substantial improvements in system efficiency and power density. Based on this perspective, three potential application scenarios are recommended: power supply for HTS magnets, HTS cable terminations, and power supply for specialised systems on spacecraft.
(3) The article identifies recent technological advancements in HTS-WPT systems and proposes future research directions. It emphasizes the necessity of reducing AC losses, developing advanced HTS material tapes, and comprehensively analyzing changes in component characteristics at cryogenic temperatures. Addressing these challenges is crucial for the further promotion and development of HTS-WPT systems.

This critical review aims to provide a comprehensive understanding of HTS-WPT systems and outline a blueprint for future research and practical applications. The main limitations involve the costs and losses associated with cooling apparatus, and the current state of HTS material manufacturing. By optimizing the operating conditions of HTS-WPT systems and selecting suitable application scenarios, these limitations can be mitigated, ultimately contributing to the realization of more efficient and sustainable WPT technologies.

## CRediT authorship contribution statement

**K.T. Chau:** Writing – original draft, Supervision, Project administration, Methodology, Funding acquisition, Conceptualization. **Wei Liu:** Writing – review & editing, Validation, Supervision. **Quan Li:** Validation, Supervision. **Rui Lyu:** Writing – review & editing, Writing – original draft, Visualization, Methodology, Investigation, Formal analysis, Data curation, Conceptualization.

## Declaration of Competing Interest

The authors declare that they have no known competing financial interests or personal relationships that could have appeared to influence the work reported in this paper.

## Data Availability

No data was used for the research described in the article.

## Acknowledgements

This work was fully supported by two grants from the Research Grants Council of the Hong Kong Special Administrative Region, China (Project No. T23-701/20-R and 17204021).

### *Declaration of generative AI and AI-assisted technologies in the writing process*

During the preparation of this work the author(s) used [GPT-4o] in order to [improve language]. After using this tool/service, the author(s) reviewed and edited the content as needed and take(s) full responsibility for the content of the publication.

## References

Andrade, V.S., Boaventura, W.C., Neves, M.A., Granados, X., 2024. Dielectric characterization of NKN in LN2 using a proposed arrangement. IEEE Trans. Appl. Supercond. 34 (3), 6600805.
Assawaworrarit, S., Yu, X., Fan, S., 2017. Robust wireless power transfer using a nonlinear parity–time-symmetric circuit. Nature 546, 387–390.
Bardeen, J., Cooper, L.N., Schrieffer, J.R., 1957. Theory of superconductivity. Phys. Rev. 108 (5), 1175.
Baros, D., Bampouras, K., Apostolidou, P., Ioannou, E., Papanikolaou, N., 2017. Multilevel inverters for motor drives and wireless power transfer applications. : Panhellenic Conf. Electron. Telecommun. (PACET). Nov 3-4; Xanthi, Greece.
Basir, A., Yoo, H., 2020. Efficient wireless power transfer system with a miniaturized quadband implantable antenna for deep-body multitasking implants. IEEE Trans. Micro Theor. Tech. 68, 1943–1953.
Beasley, M.R., Labusch, R., Webb, W.W., 1969. Flux creep in type-II superconductors. Phys. Rev. 181 (2), 682.
Bednorz, J.G., Muller, K., 1986. Possible high Tc superconductivity in the Ba-La-Cu-O system. Z. Phys. B. 64, 189–193.
Bosshard, R., Muehlethaler, J., Kolar, J., Stevanovic, I., 2013. Optimized magnetic design for inductive power transfer coils. Proc. Twenty-Eighth Annu. IEEE Appl. Power Electron. Conf. Expo. (APEC).
Bosshard, R., Kolar, J.W., Muhlethaler, J., Stevanovic, I., Wunsch, B., Canales, F., 2015. Modeling and $\eta$-$\alpha$-pareto optimization of inductive power transfer coils for electric vehicles. IEEE Trans. Emerg. Sel. Top. Power Electron 3 (1), 50–64.
Bosshard, R., Iruretagoyena, U., Kolar, J.W., 2016. Comprehensive evaluation of rectangular and double-D coil geometry for 50 kW/85 kHz IPT system. IEEE J. Emerg. Sel. Top. Power Electron 4 (4), 1406–1415.
Bourne, J., Schupbach, R., Hollosi, B., Di, J., Lostetter, A., Mantooth, H.A., 2008. Ultra-wide temperature (-230°C to 130°C) DC-motor drive with SiGe asynchronous controller. : IEEE Aerosp. Conf.
Braccini, V., Nardelli, D., Penco, R., Grasso, G., 2010. Properties of recent IBAD–MOCVD coated conductors relevant to their high field, low temperature magnet use. Supercond. Sci. Technol. 24, 035001.
Budhia, M., Covic, G.A., Boys, J.T., 2011. Design and optimization of circular magnetic structures for lumped inductive power transfer systems. IEEE Trans. Power Electron 26 (11), 3096–3108.
Budhia, M., Boys, J.T., Covic, G.A., Huang, C.Y., 2013. Development of a single-sided flux magnetic coupler for electric vehicle IPT charging systems. IEEE Trans. Ind. Electron 60 (1), 318–328.
Chen, H., Li, Q., 2020. A Comparative study of transport current loss in HTS coils for superconducting wireless power transfer. J. Phys. Conf. Ser. 1559 (1), 012010.
Chen, M., Zhang, Y., Li, X., Wu, Y., Sun, F., Zhang, H., et al., 2003. The magnetic properties of the ferromagnetic materials used for HTS transformers at 77 K. IEEE Trans. Appl. Supercond. 13 (2), 2313–2316.
Chen, R., Du, X., Zhang, X., Guo, S., Lin, H., Zhao, J., et al., 2018. Core characterization and inductor design investigation at low temperature, 2018 Sep 23-27 2018 IEEE Energy Conversion Congress and Exposition (ECCE). IEEE, Portland, OR, USA, pp. 4218–4225, 2018 Sep 23-27.
Chen, W., Liu, C., Lee, C.H., Shan, Z., 2016b. Cost-effectiveness comparison of coupler designs of wireless power transfer for electric vehicle dynamic charging. Energies 9 (906).
Chen, X.Y., et al., 2022. An ultra-low-loss superconducting inductor for power electronic circuits. IET Power Electron 15 (10), 877–885.

Chen X.Y., Jin J.X. Resonant circuit and magnetic field analysis of superconducting contactless power transfer. In: Proc Int Conf Appl Supercond Electromagn Devices. Sydney, NSW, Australia; 2011. [Online]. Available: ⟨http://ieeexplore.ieee.org/servlet/opac?punumber=6135857⟩.
Chen, X.Y., Jin, J.X., Tang, M.G., et al., 2016a. An efficient boost chopper integrated with cryogenic MOSFETs and HTS inductor. IEEE Trans. Appl. Supercond. 26 (7), 5701606.
Chen, X.Y., Zhang, M.S., Jiang, S., et al., 2021. An SMES-based current-fed transformerless series voltage restorer for DC load protection. IEEE Trans. Power Electron 36 (9), 9698–9703.
Chow, C.C.T., Ainslie, M.D., Chau, K.T., 2023. High temperature superconducting rotating electrical machines: An overview. Energy Rep. 9, 1124–1156.
Claassen, J., 2005. Inductor design for cryogenic power electronics. IEEE Trans. Appl. Supercond. 15 (2), 2385–2388.
Cota, K.A., et al., 2019. An approach for selecting compensation capacitances in resonance-based EV wireless power transfer systems with switched capacitors. IEEE Trans. Transp. Electrification 5 (4), 1004–1014.
Daniil, M., Osofsky, M.S., Gubser, D.U., Willard, M.A., 2010. (Fe, Si, Al)-based nanocrystalline soft magnetic alloys for cryogenic applications. Appl. Phys. Lett. 96 (16), 162504.
Daniil, M., Fonda, H.M., Willard, M.A., 2015. Crystal structure and magnetic properties of (Fe, Si, Al)-based nanocomposite magnets designed for cryogenic applications. Met. Mater. Trans. E. 2 (2), 139–145.
Dionne, G.F., 1997. Properties of ferrites at low temperatures. J. Appl. Phys. 81, 5064–5069.
Do Chung, Y., et al., 2013. Operating characteristics of contactless power transfer from HTS antenna to copper receiver with inserted resonator through large air gap. IEEE Trans. Appl. Supercond. 24 (3), 1–5.
Do Chung, Y., et al., 2014. Design consideration and efficiency comparison of wireless power transfer with HTS and cooled copper antennas for electric vehicle. IEEE Trans. Appl. Supercond. 25 (3), 1–5.
Do Chung, Y., et al., 2016. Design considerations of superconducting wireless power transfer for electric vehicle at different inserted resonators. IEEE Trans. Appl. Supercond. 26 (4), 1–5.
Do Chung, Y., et al., 2017. Conceptual design and operating characteristics of multi-resonance antennas in the wireless power charging system for superconducting MAGLEV train. IEEE Trans. Appl. Supercond. 27 (4), 1–5.
Do Chung, Y., et al., 2019. Operating characteristics for different resonance frequency ranges of wireless power charging system in superconducting MAGLEV train. IEEE Trans. Appl. Supercond. 29 (5), 1–5.
Do Chung, Y., Lee, C.Y., 2023. Operating characteristics of wireless multi-charging module based on multi-magnetic resonance couplings for high-speed superconducting MAGLEV train. IEEE Trans. Appl. Supercond. 33 (5), 1–6.
Dou, S.X., Soltanian, S., Horvat, J., Wang, X.L., Zhou, S.H., Ionescu, M., et al., 2002. Enhancement of the critical current density and flux pinning of MgB2 superconductor by nanoparticle SiC doping. Appl. Phys. Lett. 81, 3419–3421.
Elbuluk, M., Hammoud, A., 2005. Power electronics in harsh environments. Ind. Appl. Conf. (IAS) vol. 2, 1442–1448.
Endo, N., Nagasaki, Y., Miyagi, D., Tsuda, M., 2022. Suitable structure of tri-axial HTS cable with low thermal conductive layer for increasing power transmission cable length. IEEE Trans. Appl. Supercond. 32 (1), 4800106.
Faria, L., Passaro, A., Nohra, L., d'Amore, R., 2012. Influence of the cryogenic temperature and the BIAS voltage on the spontaneous polarization effect of X5R dielectric capacitors. Proc Int Refereed. J. Eng. Sci. 1 (1), 14–21.
Fetisov, S.S., Zubko, V.S., Zanegin, S.Y., Nosov, A.A., Vysotsky, V.S., 2021. Optimization and cold test of a triaxial 2G HTS power cable with high current capacity. IEEE Trans. Appl. Supercond. 31 (5), 5400104.
Garcia, D.F., et al., 2024. Application of 2G Coil to Increase the Voltage Gain of Boost Converters. IEEE Trans. Appl. Supercond.
Garrett, J., Schupbach, R., Mantooth, H.A., Lostetter, A.B., 2006. Development of an extreme environment DC motor drive full bridge power stage using commercial-off-the-shelf components. Int. Planet. Probe Workshop.
Gerber, S.S., Elbuluk, M.E., Hammoud, A., Patterson, R.L., 2004. Performance of high-frequency high-flux magnetic cores at cryogenic temperatures. Proc. Intersoc. Energy Convers. Eng. Conf. 249–254.
Gui, H., Wu, Y., Guo, Y., Yan, W., Fang, H., Wang, H., 2019. Review of power electronics components at cryogenic temperatures. IEEE Trans. Power Electron 35 (5), 5144–5156.
Gurevich, A., 2014. Challenges and opportunities for applications of unconventional superconductors. Annu Rev. Condens Matter Phys. 5, 35–56.
Haerinia, M., Shadid, R., 2020. Wireless power transfer approaches for medical implants: a review. Signals 1 (2), 209–229.
He, Y., Wang, Y., Nie, X., Chen, W., Yan, Z., 2018. High-temperature superconducting capacitor and its application to a superconducting wireless power transfer system. IEEE Trans. Appl. Supercond. 29 (1), 1–7.
Hirsch, J.E., Marsiglio, F., 2021. Nonstandard superconductivity or no superconductivity in hydrides under high pressure. Phys. Rev. B 103, 134505.
Huang, J., He, X., Huo, P., Xu, R., 2024. A Hybrid Modulation Strategy for LCC–LCC Compensated Bidirectional Wireless Power Transfer System to Achieve High Efficiency in the Whole Operating Range. IEEE Trans. Ind. Electron 71 (1), 327–337.
Hwang, Y.J., Jang, J.Y., 2022. Design and characteristic analysis of an inductive link for wireless current charging of a HTS magnet. IEEE Trans. Appl. Supercond. 32 (6), 1–5.
Inoue, R., et al., 2017. AC loss characteristics in kilohertz frequency band of a high-temperature superconductor coil for a wireless power transmission system. IEEE Trans. Appl. Supercond. 27 (4), 1–5.
Inoue, R., et al., 2019. Electric power transmission characteristics of a wireless power transmission system using high temperature superconducting coils for railway vehicle. IEEE Trans. Appl. Supercond. 29 (5), 1–5.
Inoue, R., et al., 2021. Thermal characteristics of REBCO coil in a wireless power transmission system for the railway vehicle in liquid nitrogen. IEEE Trans. Appl. Supercond. 31 (5), 1–5.
Inoue, R., et al., 2022b. Basic coil structure for rapid charge in a low-frequency and high-efficiency wireless power transmission system using high-temperature superconducting coil for railway vehicle. IEEE Trans. Appl. Supercond. 33 (1), 1–9.
Inoue, R., et al., 2023b. Investigation of HTS coil structure robustness against misalignment between coils in a wireless power transmission system for railway vehicles. IEEE Trans. Appl. Supercond. 33 (5), 1–5.
Inoue, R., et al., 2024. Basic experimental study on a 1 kW-class WPT system using HTS and copper coils for EVs. IEEE Trans. Appl. Supercond.
Inoue, R., Ueda, H., Kim, S., 2022a. Study on low-loss and high-energy density coil structure of a wireless power transmission system using high temperature superconducting coils for railway vehicle. IEEE Trans. Appl. Supercond. 32 (6), 1–4.
Inoue, R., Ueda, H., Kim, S., 2022c. Basic study on power transmission characteristics for high-temperature superconducting cable termination applying a wireless power transmission system. IEEE Trans. Appl. Supercond. 32 (6), 1–4.
Inoue, Y., et al., 2023a. Basic study of a wireless power transmission system using superconducting coil as a ground-side coil for electric vehicles. IEEE Trans. Appl. Supercond. 33 (5), 1–5.
Iwasa, Y., 2003. HTS magnets: stability; protection; cryogenics; economics; current stability/protection activities at FBML. Cryogenics 43 (3-5), 303–316.
Jang, J.Y., Seo, B., Hwang, Y.J., 2024. Optimal design method of a wireless charging system for HTS magnets using a genetic algorithm. IEEE Trans. Appl. Supercond.
Jeong, I.-S., Choi, H.-S., Kang, M.-S., 2015. Application of the superconductor coil for the improvement of wireless power transmission using magnetic resonance. J. Supercond. Nov. Magn. 28, 639–644.
Jeong, I.-S., Choi, H.-W., Choi, H.-S., Chung, D.C., 2018. Analysis of S-parameters using different materials for the WPT resonance coil. IEEE Trans. Appl. Supercond. 26 (3), 0500405.
Jiang, J., Bradford, G., Hossain, S.I., Brown, M.D., Cooper, J., Miller, E., et al., 2019. High-performance Bi-2212 round wires made with recent powders. IEEE Trans. Appl. Supercond. 29, 6400405.
Jones, W.K., Olmedo, R.A., Hu, Z.Q., Larkins Jr., G., 1991. Development of superconducting electrode capacitor using a YBa2 Cu3O7−x thick film and Y2BaCuO5 dielectric. IEEE Trans. Magn. 27 (2), 1619–1621.
Kamerlingh Onnes, H., 1911. The superconductivity of mercury. Comm. Phys. Lab Univ. Leiden.-. 122, 122–124.
Kamihara, Y., Watanabe, T., Hirano, M., Hosono, H., 2008. Iron-based layered superconductor La[O1-xFx]FeAs (x = 0.05-0.12) with Tc = 26 K. J. Am. Chem. Soc. 130, 3296–3297.
Kanithi, H., Blasiak, D., Lajewski, J., Berriaud, C., Vedrine, P., Gilgrass, G., 2014. Production results of 11.75 Tesla Iseult/INUMAC MRI conductor at Luvata. IEEE Trans. Appl. Supercond. 24, 1–4.
Katase, T., Ishimaru, Y., Tsukamoto, A., Hiramatsu, H., Kamiya, T., Tanabe, K., et al., 2011. Advantageous grain boundaries in iron-pnictide superconductors. Nat. Commun. 2, 409.
Kim, D.W., et al., 2013. Effect and properties of contactless power transfer for HTS receivers with four-separate resonance coils. IEEE Trans. Appl. Supercond. 23 (3), 5500404.
Kim, D.W., Chung, Y.D., Kang, H.K., Yoon, Y.S., Ko, T.K., 2012. Characteristics of contactless power transfer for HTS coil based on electromagnetic resonance coupling. IEEE Trans. Appl. Supercond. 22 (3), 5400604 (Art no.).
Kumar, Z.M., Joshi, P., Gupta, R., 2023. A 50 kA Superconducting Transformer for the Upcoming High-Field High-Current Testing Station at the BNL. IEEE Trans. Appl. Supercond. 33 (5), 5500305.
Kurs, A., Karalis, A., Moffatt, R., Joannopoulos, J.D., Fisher, P., Soljačić, M., 2007. Wireless power transfer via strongly coupled magnetic resonances. Science 317 (5834), 83–86.
Lee P. Engineering critical current density vs. applied field for superconductors. 2018. [Online]. Available: ⟨https://nationalmaglab.org/magnet-development/applied-superconductivity-center/plots⟩.
Lerosey, G., 2017. Wireless power on the move. Nature 546, 354–355.
Li, C., Wang, Z., Xu, Y., 2023. A wireless-power-transfer-based three-phase PMSM drive system with matrix converter. IEEE Trans. Ind. Electron 70 (3), 2307–2317.
Li, G.Z., Sumption, M.D., Zwayer, J.B., Susner, M.A., Rindfleisch, M.A., Thong, C.J., et al., 2013. Effects of carbon concentration and filament number on advanced internal Mg infiltration-processed $MgB_2$ strands. Supercond. Sci. Technol. 26, 095007.
Li, Q., Xin, Y., Wang, S., 2016. Dependence of AC loss on structural compactness of superconducting power cables with narrow coated conductors. IEEE Trans. Appl. Supercond. 26 (7), 5900705.
Li, S., Mi, C.C., 2015. Wireless power transfer for electric vehicle applications. J. Emerg. Sel. Top. Power Electron 3 (1), 4–17.
Li, W., et al., 2019. Quantitative comparison of wireless power transfer using HTS and copper coils. IEEE Trans. Appl. Supercond. 29 (5), 1–6.
Li, Y., et al., 2021. Extension of ZVS region of series–series WPT systems by an auxiliary variable inductor for improving efficiency. IEEE Trans. Power Electron 36 (7), 7513–7525.
Liu, J.H., Wang, Q.L., Qin, L., Zhou, B.Z., Wang, K.S., Wang, Y.H., et al., 2020. World record 32.35 tesla direct-current magnetic field generated with an all-superconducting magnet. Supercond. Sci. Technol. 33, 03LT01.

Liu, W., Chau, K.T., Chow, C.C.T., Lee, C.H.T., 2022a. Wireless energy trading in traffic internet. IEEE Trans. Power Electron 37, 4831–4841.

Liu, W., Chau, K.T., Chow, C.C.T., Lee, C.H.T., 2023. Smart wireless power transfer—opportunities and challenges. Renew. Sustain. Energy Rev. 180, 113298.

Liu, Y., Liu, C., Gao, X., Liu, S., 2022b. Design and control of a decoupled multichannel wireless power transfer system based on multilevel inverters. IEEE Trans. Power Electron 37 (8), 10045–10060.

Long, B.R., Miller, J.M., Daga, A., Schrafel, P.C., Wolgemuth, J., 2016. Which Way for Wireless Power: High Q or High K. IEEE PELS Workshop Emerg. Technol.: Wirel. Power Transf. (WoW). Jun 7-8; Knoxville, TN, USA.

Luo, Z., Wei, X., 2018. Analysis of square and circular planar spiral coils in wireless power transfer system for electrical vehicles. IEEE Trans. Ind. Electron 65 (1), 331–341.

Machura, P., Li, Q., 2019. A critical review on wireless charging for electric vehicles. Renew. Sustain Energy Rev. 104, 209–234.

Machura, P., Li, Q., 2021. AC loss reduction through flux diverters for superconducting wireless charging coils at high frequencies. IEEE Trans. Appl. Supercond. 31 (3), 1–10.

Machura, P., Kovac, J., Pospisil, J., Zou, J., Purnama, I., Kovac, P., et al., 2020. Loss characteristics of superconducting pancake, solenoid and spiral coils for wireless power transfer. Supercond. Sci. Technol. 33 (7), 074008.

Mai, R., et al., 2017. Optimization of the passive components for an S-LCC topology-based WPT system for charging massive electric bicycles. IEEE Trans. Ind. Electron 65 (7), 5497–5508.

Malinowski, M., Gopakumar, K., Rodriguez, J., Perez, M.A., 2010. A survey on cascaded multilevel inverters. IEEE Trans. Ind. Electron 57 (7), 2197–2206.

Martha's vineyard buses get wirelessly charged up with 200-kW system. 2018. [Online]. Available: 〈https://momentumdynamics.com〉.

Masuda, T., et al., 2007. Fabrication and installation results for Albany HTS cable. IEEE Trans. Appl. Supercond. 17 (2), 1648–1651.

Meissner, W., Ochsenfeld, R., 1933. Ein neuer effekt bei eintritt der supraleitfähigkeit. Naturwissenschaften 21 (44), 787–788.

Mi, C.C., Buja, G., Choi, S.Y., Rim, C.T., 2016. Modern advances in wireless power transfer systems for roadway powered electric vehicles. IEEE Trans. Ind. Electron 63, 6533–6545.

Michel, C., Hervieu, M., Borel, M.M., Grandin, A., Deslandes, F., Provost, J., et al., 1987. Superconductivity in the Bi-Sr-Cu-O system. Z. Phys. B. 68, 421–423.

Nagamatsu, J., Nakagawa, N., Muranaka, T., Zenitani, Y., Akimitsu, J., 2001. Superconductivity at 39 K in magnesium diboride. Nature 410, 63–64.

Nguyen, X.B., Vilathgamuwa, D.M., Madawala, U.K., 2014. A SiC-based matrix converter topology for inductive power transfer system. IEEE Trans. Power Electron 29 (8), 4029–4038.

Ning, P., Miller, J.M., Onar, O.C., White, C.P., 2013. A compact wireless charging system for electric vehicles. IEEE Energy Convers. Congr. Expo. (ECCE).

Obradors, X., Puig, T., 2014. Coated conductors for power applications: materials challenges. Supercond. Sci. Technol. 27, 044003.

Ogawa, J., et al., 2019. Development of an HTS capacitor using Bi2223/Ag tapes as electrodes. IEEE Trans. Appl. Supercond. 29 (5), 1–4.

Okeda, M., Sakuma, K., Sekiya, N., 2022. High efficiency wireless power transmission system that uses HTS transmitting and copper receiving coils with a large difference in quality factor. IEEE Trans. Appl. Supercond. 32 (4), 1–5.

Osabe G., Kobayashi S., Kato T., Hayashi K., Ueno E., Yamade S., et al. Recent developments of Ag-sheath Bi-2223 wire. presented at the 28th International Superconductivity Industry Summit; 2019 Sep 28; Beijing, China.

Oshimoto, N., Sakuma, K., Sekiya, N., 2023. Improvement in power transmission efficiency of wireless power transfer system using superconducting intermediate coil. IEEE Trans. Appl. Supercond. 33 (5), 1–4.

Pan, M.J., 2005. Performance of capacitors under DC bias at liquid nitrogen temperature. Cryogenics 45 (6), 463–467.

Park, C., Obadolagbonyi, O., Graber, L., 2020. Cryogenic power electronics: Capacitors and inductors. IOP Conf. Ser. Mater. Sci. Eng. 756 (1), 012010.

Parrell, J.A., Field, M., Hazen, G., Zhang, P., 2003. High field $Nb_3Sn$ conductor development at Oxford Superconducting Technology. IEEE Trans. Appl. Supercond. 13, 3470–3473.

Pasupuleti, S.S., Tummuru, N.R., Misra, H., 2023. Power management of hybrid energy storage system based wireless charging system with regenerative braking capability. IEEE Trans. Ind. Appl. 59 (3), 3785–3794.

Patil, D., McDonough, M.K., Miller, J.M., Fahimi, B., Balsara, P.T., 2018. Wireless power transfer for vehicular applications: overview and challenges. IEEE Trans. Transp. Electrific 4 (1), 3–37.

Qian, H., et al., 2019. Wireless power supply for HTS magnets: circuit topology design and cryogenic testing. IEEE Trans. Appl. Supercond. 29 (5), 1–5.

Qiu C., Chau K.T., Liu C., Chan C.C., Overview of wireless power transfer for electric vehicle charging. World Electric Vehicle Symposium and Exhibition (EVS27), Barcelona, Spain, November 2013.

Quach, H.P., Chui, T.C., 2004. Low temperature magnetic properties of Metglas 2714A and its potential use as core material for EMI filters. Cryogenics 44 (6), 445–449.

Rajashekara, K., Akin, B., 2013. A review of cryogenic power electronics: status and applications. IEEE Int. Electr. Mach. Drives Conf. (IEMDC).

Rakouth, H., et al., 2013. EV Charging Through Wireless Power Transfer: Analysis of Efficiency Optimization and Technology Trends. Springer, Berlin, Germany.

Rogalla, H., Kes, P.H. (Eds.), 2012. 100 years of superconductivity. CRC Press.

Sallán, J., et al., 2009. Optimal design of ICPT systems applied to electric vehicle battery charge. IEEE Trans. Ind. Electron 56 (6), 2140–2149.

Sato, K., Kobayashi, S., Nakashima, T., 2012. Present status and future perspective of bismuth-based high-temperature superconducting wires realizing application systems. Jpn J. Appl. Phys. 51, 010006.

Sekiya, N., et al., 2023. Wireless power transfer system using high-quality factor superconducting transmitting coil for biomedical capsule endoscopy. IEEE Trans. Appl. Supercond. 33 (5), 1–5.

Sekiya, N., Monjugawa, Y., 2017. A novel REBCO wire structure that improves coil quality factor in MHz range and its effect on wireless power transfer systems. IEEE Trans. Appl. Supercond. 27 (4), 6602005.

Sekiya, N., Sawada, M., 2023. Experimental results of ultrahigh-efficiency wireless power transfer using extremely high-quality factor superconducting coil with double-sided coated conductor tape. IEEE Trans. Appl. Supercond. 33 (3), 1–6.

Snider, E., Dasenbrock-Gammon, N., McBride, R., Debessai, M., Vindana, H., Vencatasamy, K., et al., 2020. Room-temperature superconductivity in a carbonaceous sulfur hydride. Nature 586, 373–377.

Song, K., et al., 2020. Constant current charging and maximum system efficiency tracking for wireless charging systems employing dual-side control. IEEE Trans. Ind. Appl. 56 (1), 622–634.

Song, Y., Peng, Y., Liu, D., 2021. Model-based health diagnosis for lithium-ion battery pack in space applications. IEEE Trans. Ind. Electron 68, 12375–12384.

Tesla N. The transmission of electrical energy without wires. Electrical World and Engineer. 1904.

Tesla N. Apparatus for transmitting electrical energy. US Patent. 1914;1119732.

Teyssandier, F., Prêle, D., 2010. Commercially available capacitors at cryogenic temperatures. Proc. Int Workshop Low. Temp. Electron.

Tian, X., Chau, K.T., Liu, W., 2022. Design and analysis of optimal current vector for HTS-based multi-input wireless power transfer systems. Energies 15 (12), 4337.

Tinkham M. Introduction to superconductivity. Courier Corporation; 2004.

Uglietti, D., 2019. A review of commercial high temperature superconducting materials for large magnets: from wires and tapes to cables and conductors. Supercond. Sci. Technol. 32, 053001.

ul Hassan, M., et al., 2022. Design and validation of a 20-kVA, fully cryogenic, two-level GaN-based current source inverter for full electric aircrafts. IEEE Trans. Transp. Electrification 8 (4), 4743–4759.

Utschick, C., et al., 2021. Superconducting wireless power transfer beyond 5 kW at high power density for industrial applications and fast battery charging. IEEE Trans. Appl. Supercond. 31 (3), 1–10.

Wadsworth A., Pearce M.G.S., Thrimawithana D.J. A cryogenic 3-kW GaN E-HEMT synchronous buck converter. IEEE Trans Ind Electron. 2023.

Wang, J., Li, Z., Jiang, X., Zeng, C., Shen, Z.J., 2019. Gate control optimization of Si/SiC hybrid switch for junction temperature balance and power loss reduction. IEEE Trans. Power Electron 34 (2), 1744–1754.

Weijers, H.W., et al., 2010. High field magnets with HTS conductors. IEEE Trans. Appl. Supercond. 20 (3), 576–582.

Weng T., et al. Transmission Characteristic and AC Losses of A Novel Multi-Module HTS Suspension Power Supply System. IEEE Trans Appl Supercond. 2024.

Willard, M., Heil, T., 2007. Cryogenic hysteretic loss analysis for (Fe, Co, Ni)–Zr–B–Cu nanocrystalline soft magnetic alloys. J. Appl. Phys. 101 (9), 09N113.

Wireless charging for a smooth and safe power transfer from shore to the ferry. 2019. [Online]. Available: 〈https://ipt-technology.com〉.

Wireless Power Transfer for Light-Duty Plug-In/Electric Vehicles and Alignment Methodology. Standard SAE J2954; 2016.

Wu, M.K., Ashburn, J.R., Torng, C.J., Hor, P.H., Meng, R.L., Gao, L., et al., 1987. Superconductivity at 93 K in a new mixed-phase Y-Ba-Cu-O compound system at ambient pressure. Phys. Rev. Lett. 58, 908–910.

Xiao, L.Y., Dai, S.T., Lin, L.Z., Zhang, J.Y., Guo, W.Y., Zhang, D., et al., 2012. Development of the world's first HTS power substation. IEEE Trans. Appl. Supercond. 22, 5000104.

Xiao, X.Y., Liu, Y., Jin, J.X., Li, C.S., Xu, F.W., 2016. HTS applied to power system: Benefits and potential analysis for energy conservation and emission reduction. IEEE Trans. Appl. Supercond. 26 (7), 5403309.

Yao, C., Ma, Y., 2021. Superconducting materials: Challenges and opportunities for large-scale applications. iScience 24, 103.

Yao, C., Lin, H., Zhang, Q.J., Zhang, X.P., Wang, D.L., Dong, C.H., et al., 2015. Critical current density and microstructure of iron sheathed multifilamentary Sr1-xKxFe2As2/Ag composite conductors. J. Appl. Phys. 118, 203909.

Yazdani-Asrami, M., Sadeghi, A., Atrey, M.D., 2022. Selecting a cryogenic cooling system for superconducting machines: General considerations for electric machine designers and engineers. Int J. Refrig 140, 70–81.

Yoo, B., Song, J.-B., Kim, J.C., Kim, Y.-G., Kim, J., Sim, K., Shin, I., Hwang, D.Y., Lee, H., 2018. Superconducting properties of reacted mono- and multifilament MgB2 wires with respect to bending diameters using a custom-made bending test probe. IEEE Trans. Appl. Supercond. 28 (3).

Yu, H., et al., 2018. Asymmetry in wireless power transfer between a superconducting coil and a copper coil. IEEE Trans. Appl. Supercond. 28 (3), 1–6.

Yu, H., Zhang, G., Liu, G., Liu, Q., Jing, L., 2019. Wireless power transfer using a superconducting capacitor. Phys. C. Supercond. Appl. 562, 85–89.

Yuan, J., Shen, G.X., 2004. Quality factor of Bi (2223) high-temperature superconductor tape coils at radio frequency. Supercond. Sci. Technol. 17, 333–336.

Zaheer, A., et al., 2014. Investigation of multiple decoupled coil primary pad topologies in lumped IPT systems for interoperable electric vehicle charging. IEEE Trans. Power Electron 30 (4), 1937–1955.

Zhang, G.M., Wang, X.N., Li, Y.H., Chen, Z.P., Li, P., Zhang, J., 2013. Wireless power transfer using high temperature superconducting pancake coils. IEEE Trans. Appl. Supercond. 24 (3), 1–5.

Zhang, H., Peng, Y., Liu, D., Wang, X., Li, X., Chen, J., 2021b. Alternating current loss of superconductors applied to superconducting electrical machines. Energies 14, 2234.
Zhang, W., et al., 2014. Load-independent duality of current and voltage outputs of a series-or parallel-compensated inductive power transfer converter with optimized efficiency. IEEE J. Emerg. Sel. Top. Power Electron 3 (1), 137–146.
Zhang, Y., et al., 2018. Modeling and analysis of a strongly coupled series–parallel-compensated wireless power transfer system. IEEE J. Emerg. Sel. Top. Power Electron 7 (2), 1364–1370.
Zhang Y.F. 2G HTS wire production at SuperPower for emerging magnet applications. presented at the 28th International Superconductivity Industry Summit; 2019 Sep 28; Beijing, China.
Zhang, Z., Wang, D.L., Wei, S.Q., Wang, Y.Z., Wang, C.T., Zhang, Z., et al., 2021a. First performance test of the iron-based superconducting racetrack coils at 10 T. Supercond. Sci. Technol. 34, 035021.
Zhao, B., Song, Q., Liu, W., Sun, Y., 2014. Overview of dual-active-bridge isolated bidirectional DC–DC converter for high-frequency-link power-conversion system. IEEE Trans. Power Electron 29, 4091–4106.
Zhao, Z.X., Chen, L.Q., Yang, Q.S., Huang, Y.Z., Chen, G.H., Tang, R.M., et al., 1987. Superconductivity above liquid nitrogen temperature in new oxide system. Sci. Bull. 32, 1098–1102.
Zheng, Z., et al., 2023. An ultralow-loss fault-current-limiting Z-Source LVDC circuit breaker using cryogenic power electronics. IEEE Trans. Power Electron 38 (5), 5626–5633.
Zhou, P., et al., 2020. A contactless self-regulating HTS flux pump. IEEE Trans. Appl. Supercond. 30 (4), 1–6.
Zuo, W., et al., 2014. Investigation of efficiency and load characteristics of superconducting wireless power transfer system. IEEE Trans. Appl. Supercond. 25 (3), 1–6.

**K. T. Chau** received the B.Sc. (Eng.), M.Phil., and Ph.D. degrees in electrical and electronic engineering from The University of Hong Kong, Hong Kong, in 1988, 1991, and 1993, respectively. Currently, he serves as Chair Professor of Electrical Energy Engineering at the Research Centre for Electric Vehicles and Department of Electrical and Electronic Engineering, The Hong Kong Polytechnic University. His research interests include electric and hybrid vehicles, power electronics and drives, and renewable energies. He is the author of nine books and more than 350 journal papers.Prof. Chau is a Fellow of the Institution of Engineering and Technology (IET), U.K., and of the Hong Kong Institution of Engineers. He is also a Co-editor of the Journal of Asian Electric Vehicles. He is a Chartered Engineer. He was the recipient of the Changjiang Chair Professorship from the Ministry of Education, China, and the Environmental Excellence in Transportation Award for Education, Training, and Public Awareness from the Society of Automotive Engineers International.